Enhanced expression of the human *Survival motor neuron 1* gene from a codon-optimised cDNA transgene *in vitro* and *in vivo*

Neda A.M. Nafchi[1]*, Ellie M. Chilcott[1]*, Sharon Brown[2,3], Heidi R. Fuller[2,3], Melissa Bowerman[3,4] and Rafael J. Yáñez-Muñoz[1].

[1] AGCTlab.org, Centre of Gene and Cell Therapy, Centre for Biomedical Sciences, Department of Biological Sciences, School of Life Sciences and Environment, Royal Holloway University of London, TW20 0EX, UK.

[2] School of Pharmacy and Bioengineering, Keele University, Staffordshire, ST5 5BG, UK.

[3] Wolfson Centre for Inherited Neuromuscular Disease, TORCH Building, RJAH Orthopaedic Hospital, Oswestry SY10 7AG, UK.

[4] School of Medicine, Keele University, Staffordshire, ST5 5BG UK.

*These authors contributed equally to this work.

Corresponding author:

Prof. Rafael J. Yáñez-Muñoz

Email: rafael.yanez@royalholloway.ac.uk

Abstract

Spinal muscular atrophy (SMA) is a neuromuscular disease particularly characterised by degeneration of ventral motor neurons. *Survival motor neuron* (*SMN*) *1* gene mutations cause

SMA, and gene addition strategies to replace the faulty *SMN1* copy are a therapeutic option. We have developed a novel, codon-optimised *hSMN1* transgene and produced integration-proficient and integration-deficient lentiviral vectors with cytomegalovirus (CMV), human synapsin (hSYN) or human phosphoglycerate kinase (hPGK) promoters to determine the optimal expression cassette configuration. Integrating, CMV-driven and codon-optimised *hSMN1* lentiviral vectors resulted in the highest production of functional SMN protein *in vitro*. Integration-deficient lentiviral vectors also led to significant expression of the optimised transgene and are expected to be safer than integrating vectors. Lentiviral delivery in culture led to activation of the DNA damage response, in particular elevating levels of phosphorylated ataxia telangiectasia mutated (pATM) and γH2AX, but the optimised *hSMN1* transgene showed some protective effects. Neonatal delivery of adeno-associated viral vector (AAV9) vector encoding the optimised transgene to the $Smn^{2B/-}$ mouse model of SMA resulted in a significant increase of SMN protein levels in liver and spinal cord. This work shows the potential of a novel codon-optimised *hSMN1* transgene as a therapeutic strategy for SMA.

Introduction

Spinal muscular atrophy (SMA) is an autosomal recessive neuromuscular disease chiefly characterised by degeneration of motor neurons from the ventral horn of the spinal cord. *Survival motor neuron* (*SMN*) *1* gene is the SMA-determining gene, being absent in 95% patients and mutated in the remaining 5% (1). *SMN2* is a highly similar gene with only five nucleotide mismatches, which result in 90% truncated transcripts lacking exon 7 (*SMNΔ7*) (2, 3), producing only low levels of SMN protein. *SMN2* copy number is a strict determinant of disease severity, whereby patients with only two copies of the gene present with the severe type I form of SMA while patients with a greater number of *SMN2* copies have less severe symptoms (4-6). Full-length SMN is a ubiquitous and essential cellular protein that has roles in RNA

metabolism, cytoskeletal maintenance, transcription, cell signaling and DNA repair (7). For many years, it was thought that motor neurons were the only affected cells, but recent evidence suggests a wide range of systemic pathologies are also caused by low levels of SMN protein. Therefore, an effective and successful therapy for SMA is likely to involve the consideration of SMA as a multi-system disorder (8, 9).

In the past five years, three therapies for SMA patients have been approved by regulatory bodies: Spinraza, Zolgensma and Evrysdi, the first two of which are genetic therapies. Spinraza is an antisense oligonucleotide that increases the level of full-length SMN protein by binding and altering the splicing of *SMN2* pre-mRNA (10), enhancing the inclusion of exon 7 (11). Zolgensma is an adeno-associated viral vector of serotype 9 (AAV9) vector containing the cDNA of the human *SMN1* gene under the control of the cytomegalovirus enhancer/chicken-β-actin-hybrid promoter (12). Evrysdi is a small molecule that modulates *SMN2* RNA splicing by binding to two unique sites in *SMN2* pre-mRNA: 5′ splice site of intron 7 and an exonic splicing enhancer 2 in exon 7, therefore promoting inclusion of exon 7 (13). Evrysdi is an oral medicine expected to be taken for the duration of the individual's life (13), while Spinraza requires repeated delivery through intrathecal injections and Zolgensma is a one-off intravenous infusion.

Gene therapy is a technology that allows the modification of gene expression with one possible strategy being the introduction of transgenes for therapeutic purposes. In this context, the efficient delivery of therapeutic genes, or other gene therapy agents, is a critical requirement for the development of an effective treatment. Vectors derived from lentiviruses have proven to be efficient gene delivery vehicles as they integrate into the host's chromosomes and show continued expression for a long time (14). They also have a relatively large cloning capacity, which is sufficient for most clinical purposes (15, 16). Lentiviral vectors can transduce different types of cells, including quiescent cells, have low immunogenicity upon *in vivo* administration,

lead to stable gene expression and can be pseudotyped with alternative envelopes to alter vector tropism (17).

Due to their unique advantages, lentiviral vectors are important gene delivery systems for research and clinical applications (16). Lentiviral vectors have been utilised to treat symptoms in several animal models, such as X-linked severe combined immunodeficiency (SCID-X1) (18), β-thalassemia (19), Wiskott-Aldrich syndrome (20), metachromatic leukodystrophy (21), haemophilia (22), Fanconi anaemia (23) and liver disease (24), as well as being used in clinical applications (25-27). Although the integrative nature of lentiviral vectors provides long-term transgene expression, integration events carry the risk of insertional mutagenesis (28-30). Intensive study of the genome and analysis of integration strategies of lentiviral vectors has led to the development of a number of strategies to minimise these risks. These include the use of viral vectors with a safer integration pattern, the utilisation of self-inactivating vectors and the design of integration-deficient lentiviral vectors (IDLVs). IDLVs are non-integrative due to an engineered class I mutation in the viral *integrase* gene, most commonly involving an amino acid change at position D64 within the catalytic core domain (31).

Here, we show the development of an integration-deficient lentiviral system expressing a novel, sequence ("codon")-optimised cDNA transgene, *Co-hSMN1*, which leads to effective SMN production in primary cultures and rescue of nuclear gems, distinct and punctate nuclear bodies where the SMN protein localises in high concentrations. Rescue of SMN production was also seen in an SMA type I induced pluripotent stem cell (iPSC)-derived motor neuron (MN) model. *In vivo* data showed that an AAV9 vector expressing this transgene could strongly restore SMN protein production in the *Smn*$^{2B/-}$ SMA mouse model (32). We also found that untreated SMA cells exhibit molecular signatures of DNA damage with prominent γH2AX foci and a trend for increased pATM expression. Notably, IDLV_*Co-hSMN1* was able to reverse an initial spike in

pATM signaling, suggesting some protective effect. Together, these data point to novel benefits of gene therapy for SMA, and importantly, highlight an alternative transgene and delivery system.

Materials and methods

Optimisation of hSMN1 sequence

The wild-type cDNA sequence of the human *SMN1* transcript was codon-optimised using custom services provided by GeneArt/ThermoFisher Scientific to generate *Co-hSMN1*. The GeneArt algorithm identifies and optimises a variety of factors relevant to different stages of protein production, such as codon adaptation, mRNA stability, and various *cis* elements in transcription and translation to achieve the most efficient expression. This transgene was then cloned into lentiviral and AAV transfer plasmid using standard molecular biology procedures.

Fibroblast cell culture

Low passage, primary human fibroblasts from wild-type (GM04603) and SMA type I (GM00232) donors were obtained from Coriell Institute for Medical Research and used to assess overall lentiviral transduction efficiency, γH2AX and caspase 3 foci, and ATM and pATM levels. Similar wild-type and SMA type I fibroblast cell lines were also obtained from E. Tizzano (33) and used to assess restoration of gems following transduction. All fibroblasts were cultured in 65% DMEM+Glutamax, 21% M199, 10% FBS, 10 ng/ml FGF2, 25 ng/ml EGF and 1 µg/ml gentamicin.

Isolation and culture of E18 mouse cortical neurons

Preparation of primary cortical cultures from E18 mouse embryos followed the protocol described in Lu-Nguyen *et al* (34).

Preparation of embryonic rat motor neuron primary cultures

The isolation and culture of primary rat motor neurons was achieved by following the protocol previously described in Peluffo et al (35).

iPSC culture and motor neuron differentiation

Six iPSC lines were used in this project; three wild-type (4603, derived in house from GM04603 fibroblasts (33); 19-9-7T, from WiCell and AD3-CL1, gifted by Majlinda Lako) and three SMA type I (SMA-19, gifted by Majlinda Lako; CS13iSMAI-nxx and CS32iSMAI-nxx, obtained from Cedars-Sinai). Undifferentiated iPSCs were seeded at a density of 20,000 cells/cm^2 onto Matrigel-coated cultureware in mTeSR™1 or mTeSR™ Plus media for general growth.

iPSCs were grown until 90% confluent in 6 well plates then clump passaged with 0.5mM EDTA to Matrigel-coated 10cm dishes until 60-70% confluent. A protocol adapted from Maury et al (36) was used to differentiate iPSCs into MNs. Basal medium (1X DMEM/F12, 1X Neurobasal, 1X B27, 1X N2, 1X antibiotic-antimycotic, 1X *β*-mercaptoethanol and 0.5 µM ascorbic acid) was used throughout the 28-day protocol. Basal medium was supplemented at specific stages with additional compounds: 3 µM Chir99021 (days 0-3), 1 µM Compound C (days 0-3), 1 µM retinoic acid (day 3+), 500 nM SAG (day 3+), 0.5 µg/ml laminin (day 16+), 10 ng/ml each of IGF1, CNTF, BDNF, GDNF (all day 16+) and 10 µM DAPT (days 16-23). Single cell passaging on days 9, 13 (1:3 split ratio) and 16 (at appropriate density for final assay) was performed using Accutase and cells were re-seeded onto Matrigel-coated cultureware in the presence of 10 µM ROCK inhibitor for 24 hours.

Viral vector production

A 3rd generation, transient transfection system was used to generate self-inactivating HIV-1-based lentiviral vectors by calcium phosphate co-transfection of HEK293T/17 cells with pMDLg/pRRE or pMDLg/pRRE_intD64V (for integrating and non-integrating vectors, respectively), pRSV_REV, pMD2_VSV-G and a transfer plasmid containing the promoter of interest and either *hSMN1*, *Co-hSMN1* or *eGFP* at a 1:1:1:2 ratio, respectively. Supernatants were harvested at 48- and 72-hours post-transfection and lentiviral vectors were concentrated by ultracentrifugation. Vectors were titrated by qPCR and where possible, by flow cytometry (31).

AAV_CAG_*Co-hSMN1* and AAV_CAG_*eGFP* vectors were commercially produced by Atlantic Gene Therapies (France) and were titrated by qPCR against the inverted terminal repeats (ITRs).

Viral transduction in cell culture

For transduction of cell lines and primary fibroblasts, cells were seeded in appropriate media 24 hours prior to transduction. Lentiviral vectors were diluted in fresh media at the desired qPCR MOI then added to cells in the minimum volume needed to cover cells. 1 hour after transduction, media was topped up to an appropriate volume. All cells were incubated for 72-hours before analysis. Fibroblasts were transduced in the presence of 2 µg/ml polybrene. iPSC-derived MNs were transduced at day 28 of differentiation to ensure maturity of cells.

Transduction of primary motor neurons was carried out 2 hours post-seeding, while for primary cortical neurons it was three weeks post-seeding. Lentiviral vectors were diluted in conditioned media at the desired qPCR MOI. Analyses were performed three days post-transduction.

Viral transduction in vivo

Single-stranded AAV9 vectors (AAV9_CAG_*Co-hSMN1* & AAV9_CAG_*eGFP*) were administered intravenously through the facial vein to post-natal day (P) 0 $Smn^{2B/-}$ SMA mice at a dose of 8E10 vg/pup. Liver and spinal cord were harvested at P18 from untreated $Smn^{2B/-}$ mice (n=6), $Smn^{2B/-}$ mice treated with AAV9_CAG_*eGFP* (n=5) or AAV9_CAG_*Co-hSMN1* (n=5) and age-matched wild-type controls (n=4). At P18 there are overt symptoms in untreated $Smn^{2B/-}$ mice.

Experimental procedures were authorized and approved by the Keele University Animal Welfare Ethical Review Body (AWERB) and UK Home Office (Project Licence P99AB3B95) in accordance with the Animals (Scientific Procedures) Act 1986.

RT-PCR

An RT-PCR was performed using cDNA extracted from SMA iPSC MNs to identify the origins of *SMN* transcripts. The primers used to amplify a region between exons 6-8 of the *SMN* genes, plus β-actin and GAPDH as housekeeping genes were as follows: Exon6_F CTCCCATATGTCCAGATTCTCTTG, Exon8_R CTACAACACCCTTCTCACAG, β-actin_F TCACCCACACTGTGCCCATCTACGA, β-actin_R CAGCGGAACCGCTCATTGCCAATGG, 189_mGapdhex4_Fw AAAGGGTCATCATCTCCGCC, 190_mGapdhex4-5_Rv ACTGTGGTCATGAGCCCTTC. *SMN* RT-PCR amplicons were digested with *Dde*I to reveal *FL-SMN1* (504bp), *FL-SMN2* (382+122bp) and *SMN2Δ7* (328+122bp) transcripts.

Immunofluorescence

Fibroblasts were fixed with 4% PFA before being concurrently permeabilised and blocked in 5% normal goat serum in PBS with 0.25% Triton X-100. Primary and secondary antibodies were incubated with samples overnight at 4°C or 1 hour at room temperature, respectively. iPSC MNs were seeded at a density of 25,000 cells on day 16 of differentiation onto 13 mm coverslips coated with 15 µg/ml poly-ornithine and Matrigel. 4% PFA and 5% normal goat serum in PBS with 0.25% Triton X-100 were used to fix, permeabilise and block coverslips before antibody incubation at room temperature for both primary (2 hours) and secondary (1 hour). All cells were counterstained with 1 µg/ml DAPI, mounted using Fluoromount™ Aqueous mounting medium then imaged using a Zeiss Axio Observer D1 fluorescent microscope (Germany).

Primary antibodies: anti-gemin2 (Abcam, ab6084, 2.5 µg/ml), anti-SMN (BD Biosciences, 610646, 0.6 µg/ml), anti-OLIG2 (Santa Cruz, sc-515947, 2 µg/ml), anti-SMI-32 (Biolegend, 801701, 10 µg/ml), anti-*β*III-tubulin (Sigma, T2200, 10 µ/ml), anti-choline acetyltransferase (Abcam, ab181023, 5.4 µg/ml), anti-HB9 (DSHB, 81.5c10, 1:50). Secondary antibodies: goat anti-mouse IgG Alexa Fluor 488 (Invitrogen, A-11001, 2 µg/ml), goat anti-mouse IgG Alexa Fluor 555 (Invitrogen, A-21424, 2 µg/ml), goat anti-rabbit IgG Alexa Fluor 488 (Invitrogen, A-11034, 2 µg/ml).

Measurement of SMN intensity by immunofluorescence

Analyses of all samples was performed blind to vector type, gene of interest and MOI. Fluorescence pixel intensities (background corrected) were measured in a region of interest around the motor neuron cell body and are expressed as arbitrary units (a.u.) per μm^2.

Western blotting

Cultured cells were lysed in RIPA buffer supplemented with Halt Protease Inhibitor Cocktail and Phosphatase Inhibitor Cocktail 3 and the concentration of resulting protein lysates was determined using the Bio-Rad DC protein assay according to manufacturer's instructions. SMN western blots used 4-15% Tris-Glycine gels and PageRuler™ Plus Prestained Protein Ladder, whilst ATM and phosphorylated ATM western blots used NuPAGE™ 3-8% Tris-Acetate gels and HiMark™ Pre-stained protein standard. Western blots containing samples from iPSC MNs were subjected to total protein staining immediately after transfer using REVERT Total Protein Stain and Wash, as per manufacturer's instructions. Nitrocellulose membranes were blocked in an appropriate buffer (Intercept® 1:1 PBS, 5% milk/PBS or 5% BSA/PBS) for 1 hour at room temperature. Primary and secondary antibodies were diluted in blocking buffer 0.1% Tween-20, with incubations overnight at 4°C or 1 hour at room temperature, respectively. Western blots were imaged using the Odyssey CLx (LI-COR Biosciences, US) in 700nm and 800nm channels. Quantification of protein signals was achieved using Image Studio Lite.

Primary antibodies: anti-SMN (BD Biosciences, 610646, 0.05 µg/ml), anti-ATM (Abcam, ab32420, 0.12 µg/ml), anti-ATM phospho (Abcam, ab81292, 0.28 µg/ml), anti-alpha tubulin (Abcam, ab4074, 0.33 µg/ml). Secondary antibodies: IRDye 800CW goat anti-mouse IgG (LiCor, 926-32210, 0.5 µg/ml), goat anti-rabbit IgG Alexa Fluor 680 (Invitrogen, A-21076, 0.4 µg/ml).

Western blots were carried out on liver and spinal cord tissues from *Smn*$^{2B-/-}$ mice, which were extracted as previously described (37) using 2X modified RIPA buffer (2% NP-40, 0.5% deoxycholic acid, 2 mM EDTA, 300 mM NaCl and 100 mM Tris-HCl (pH 7.4)). Firstly, the tissues were diced and added to the extraction buffer and homogenized with pellet pestles, then, after 5 minutes on ice, the tissues were sonicated at 5 microns for 10 s. This process was repeated a further 2 times. The tissue extracts were centrifugated at 13,000 RPM (MSE,

Heathfield, UK; MSB010.CX2.5 Micro Centaur) for 5 minutes at 4°C and their protein concentrations calculated using a BCA protein assay (PierceTM, 23227). Following adjustment of protein levels, the tissue extracts were heated for 3 minutes at 95°C in 2X SDS sample buffer (4% SDS, 10% 2-mercaptoethanol, 20% glycerol, 0.125 M Tris-HCl (pH 6.8) and bromophenol blue) then loaded onto 4-12% Bis-Tris polyacrylamide gels for SDS-PAGE. The gel was excised along the horizontal axis at a molecular weight greater than that expected for SMN (38 kDa) and the proteins in the lower half of the gel were transferred onto a nitrocellulose membrane overnight via western blot then blocked with 4% powdered milk in PBS. The membranes were probed for SMN with the mouse anti-SMN antibody (MANSMA12 2E6 (38)), at either 1:50 or 1:100 for 2 hours and subsequently incubated with HRP-labelled rabbit anti-mouse Ig (DAKO, P0260) at 0.25 ng/ml for 1h. Both incubations were at room temperature and antibodies prepared in diluent (1% FBS, 1% horse serum (HS), 0.1% bovine serum albumin (BSA) in PBS with 0.05% Triton X-100). Following incubation with West Pico, SMN-positive bands were imaged with the Gel Image Documentation system (Bio-Rad). Total protein was assessed in the upper half of the gel via Coomassie blue staining, and this data was used as the internal loading control for each sample. ImageJ Fiji software (v1.51; (39)) was used to analyse both antibody reactive and Coomassie-stained gel bands.

Statistical analyses

Data are presented as mean ± standard deviation. For all experiments where replicate data are presented, at least n = 3 biological replicates were used, unless otherwise stated in specific sections. A range of statistical tests were used, with the most appropriate test for each dataset being determined individually. Data were tested for a normal distribution wherever possible, and appropriate parametric and non-parametric tests were used accordingly.

Results

Lentiviral and AAV9 vectors used for over-expression of hSMN1

To test whether production of SMN could be improved by codon-optimisation of *hSMN1*, we used a wild-type *hSMN1* cDNA and engineered an optimised form using a customised commercial procedure. A comparison of wild-type and *Co-hSMN1* cDNAs is shown in Fig. S1. Both cDNAs were cloned into several lentiviral plasmid backbones under the control of CMV, hSYN and hPGK promoters and in all cases, followed by a mutated form of the WPRE sequence (to prevent putative expression of woodchuck hepatitis virus X protein; Fig. 1A-C). These transfer plasmids were used to produce integrating and integration-deficient lentiviral vectors. Finally, the *Co-hSMN1* transgene was also cloned into an AAV plasmid backbone under the control of the CAG promoter, followed by a mutated WPRE element (Fig. 1E). This plasmid, as well as a control AAV_CAG_*eGFP* plasmid (Fig. 1F), was used to produce single-stranded AAV9 vectors for *in vivo* use.

Over-expression of codon-optimised hSMN1 *in primary neuronal cultures*

Mouse cortical neuron cultures and rat motor neuron cultures were characterised as shown in Fig. S2, demonstrating the expected morphology and the presence of relevant markers. Integration-proficient (IPLV) and integration-deficient (IDLV) lentiviral vectors driven by the CMV or hSYN promoters, encoding either wild-type *hSMN1* or the novel codon-optimised *Co-hSMN1* transgene were used to transduce the cultures (Fig. 2). Dose-dependent increases in mean SMN fluorescence intensity were seen by western blot in cortical neurons and immunofluorescence in motor neurons (Fig. 2B,D and Tables S1,2). IPLV delivery led to higher expression levels than with IDLVs, but SMN protein levels from the latter were also considerably

elevated. In terms of the promoter, CMV resulted in higher SMN levels regardless of vector integration proficiency. The codon-optimised transgene led to significant increases in SMN production in all cases, highlighting the improvements that this technology can afford for transgenic gene expression.

Characterisation of Co-hSMN1 *IDLVs in human iPSC-derived MNs*

Three different wild-type and three SMA type I iPSC clones were differentiated into MNs with high efficiency, exhibiting a characteristic neural network and individual cellular morphology (Fig. 3A) with >90% OLIG2 positive MN progenitors at day 16 and 77.3% SMI-32-, 61.4% HB9- and 90.1% ChAT-positive MNs at maturity (Fig. S3). A lack of full-length *SMN1* transcripts (Fig. S4) and an 18-fold reduction in SMN protein (Fig. S4) were evident in SMA type I MNs compared to wild-type cells ($P<0.0001$).

Transduction of SMA type I iPSC-derived MNs with IDLV_*Co-hSMN1* driven by CMV, hSYN or PGK promoters led to an increase in SMN protein levels, detected by both immunofluorescence (Fig. 3B) and western blot (Fig. 3C,D). Quantitation of western blot data showed that SMN protein was increased in all transduced samples compared to untransduced counterparts (Fig. 3D). IDLVs expressing *Co-hSMN1* under the transcriptional control of either CMV or hPGK promoters were able to significantly increase SMN protein production in all iPSC MN lines (Fig. 3D), whereas IDLV_hSYN_*Co-hSMN1* only led to a significant increase in CS13iSMAI-nxx. Maximal SMN protein levels were observed with IDLVs expressing *Co-hSMN1* under the transcriptional control of CMV (line SMA-19: 79.8-fold, $P<0.0001$; CS13iSMAI-nxx: 14.5-fold, $P<0.0001$; CS32iSMAI-nxx: 42.8-fold, $P<0.0001$). When levels were compared to those in wild-type iPSC MNs, supraphysiological SMN protein was evident in SMA-19 and CS32iSMAI-nxx lines, but not in CS13iSMAI-nxx.

Transduction and rescue of human SMA type I fibroblasts by lentiviral vectors encoding Co-hSMN1

Cultured human wild-type or type I SMA fibroblasts were transduced with IDLVs encoding wild-type or *Co-hSMN1* under CMV, hSYN or hPGK promoters. A clear increase in cytoplasmic SMN was seen by immunofluorescence in both wild-type and SMA type I fibroblasts following IDLV transduction (Fig. 4A) and a statistically significant increase was confirmed by western blot (Fig. 4B,C). Analysis of total SMN levels in transduced fibroblasts (Fig. 4C) corroborated the pattern of expression seen in SMA type I iPSC-MNs (Fig. 3D), where CMV-driven vectors were able to increase SMN expression to the highest extent, followed by hPGK and then hSYN-driven vectors.

SMA type I fibroblasts were transduced with IPLVs and IDLVs to determine the effectiveness of each vector to restore SMN-expressing nuclear gems, which are largely absent in SMA type I samples. All vectors were able to restore the presence of gems in transduced cells (Fig. 5A and Table S3) in an MOI-dependent manner (Fig. 5B). At the highest MOI tested (MOI 100), no visible changes in cell morphology were seen, suggesting absence of vector-mediated toxicity. IPLV transduction led to a 1.6-fold greater number of gems than in IDLV-transduced cells ($P=0.0015$), regardless of promoter or transgene (Fig. 5B). Moreover, *Co-hSMN1* led to the restoration of a significantly higher number of gems than wild-type *hSMN1* (1.7-fold, $P=0.0005$). With regards to choosing the optimal promoter, CMV-driven vectors were able to increase gem number by 1.8-fold compared to hSYN-driven vectors ($P= 0.0003$). In some cases, a higher number of gems was seen in transduced SMA type I fibroblasts than in healthy cells.

Analysis of downstream DNA damage markers following in vitro *IDLV transduction*

The molecular links between SMN and DNA damage- and apoptosis-related proteins (40-43) are not completely clear but learning how SMN interacts with these pathways may be important in understanding why SMA MNs degenerate and how this could be modulated by treatment with an *SMN*-encoding vector. It is also important to understand the consequences of SMN restoration to wild-type or supraphysiological levels, and what effect this might have on cells that have always been severely deficient in SMN.

γH2AX foci are hallmarks of DNA damage (44, 45) and immunofluorescent detection of these in untreated wild-type and SMA type I fibroblasts revealed distinct foci in nuclei of both genotypes, but these were seen more frequently in SMA type I cells (Fig. 6A). Both the number of foci per cell and the percentage of cells exhibiting any number of foci were significantly higher in SMA type I samples (Fig. 6B,C; P=0.0057 and P=0.0069, respectively). Upon transduction of SMA type I fibroblasts with IDLV_CMV_*Co-hSMN1* (the IDLV vector shown to be most potent in previous experiments), signs of DNA damage were increased further as the number of γH2AX foci, and γH2AX foci-positive cells increased significantly, compared to mock-treated SMA type I cells (Fig. 6B,C; P=0.0134 and P=0.0068, respectively). At this stage, it is unclear whether this increase was due to the act of lentiviral transduction, or due to a sudden increase in SMN levels in cells that had always been deficient. Of note, no increase in levels of cleaved caspase 3, a marker of DNA damage and apoptosis (46), was observed in IDLV_*Co-hSMN1*-transduced SMA type I fibroblasts (Fig. S5).

ATM, specifically its phosphorylated form, acts as a chief mobiliser of cellular DNA damage and apoptotic pathways that may be active in SMA cells (47). Levels of total ATM were found to be equal in both wild-type and SMA type I fibroblasts according to quantitated western blots (Fig. 7A; P=0.6662 and Fig. S6), with the phosphorylated form only showing a trend for increased

signal in the mutant cells (Fig. 7B; P>0.05). Phosphorylated ATM could be significantly increased by treatment of the cells with 200 μM hydrogen peroxide for 2 hours (Fig. 7B; wild-type vs SMA+H_2O_2 P<0.01, SMA vs SMA+H_2O_2 P<0.05). Following transduction of SMA type I fibroblasts with either IDLV_CMV_*eGFP* or IDLV_CMV_*Co-hSMN1*, phosphorylated ATM was assessed. At 3 days post-transduction, pATM was significantly increased in IDLV_CMV_*eGFP* treated cells, but not in IDLV_CMV_*Co-hSMN1* (Fig. 7C; P=0.0160 and P=0.4983, respectively). pATM remained relatively high in IDLV_CMV_*eGFP* treated cells at 7 days post-transduction (Fig. 7C; P=0.0002), whereas in IDLV_CMV_*Co-hSMN1*-transduced cells dropped below that of mock samples (Fig. 7C; P=0.0256). ATM and pATM levels were also measured in SMA type I iPSC-derived MNs, mock-transduced or treated with IDLV_CMV_*Co-hSMN1*. No effect of transduction on total ATM was observed, but a significant increase in pATM was seen in two out of three SMA type I iPSC-MN lines at 3 days post-transduction (Fig. 7D,E; SMA-19 P<0.0001, CS13iSMAI-nxx P=0.0003, CS32iSMAI-nxx P=0.0160).

Together, these data show that at least two markers of DNA damage are increased in the short-term window following lentiviral transduction of SMA cells. As pATM levels then normalised again, and were even reduced to below those of untreated cells, we suggest that this short-term increase in DNA damage markers is due to the act of transduction, rather than our *Co-hSMN1* transgene. Although γH2AX foci were not measured at later time points, we suspect this outcome measure would follow the same pattern.

In vivo *expression from AAV_CAG_*Co-hSMN1 *in the* $Smn^{2B/-}$ *mouse model of SMA*

To test the expression of *Co-hSMN1 in vivo*, we chose the *$Smn^{2B/-}$* mouse model of SMA, where over-expression of the transgene would be easily detected above low background levels of the protein. An AAV9 vector driven by the CAG promoter and including a mutated WPRE element

was produced, and an AAV9_CAG_*eGFP* vector used as a control. These vectors were delivered to neonatal mice and SMN expression assessed in liver and spinal cord samples harvested at the symptomatic time-point of P18.

Livers of untreated and AAV9_CAG_*eGFP*-treated $Smn^{2B/-}$ mice showed significantly less SMN than wild-type controls (Fig. 8A,B; P=0.0377 and P=0.0118, respectively), whereas those treated with AAV9_CAG_*Co-hSMN1* exhibited 1.7-fold of wild-type levels (Fig. 8A,B; SMN vs wild-type P=0.0725, SMN vs $Smn^{2B/-}$ P=0.0005). Data from spinal cord samples showed similarly low levels of SMN in $Smn^{2B/-}$ mice, and more variability in AAV9_CAG_*Co-hSMN1* treated mice, but a 2.6-fold increase above wild-type SMN levels was still seen (Fig. 8C,D; SMN vs wild-type P=0.5260, SMN vs $Smn^{2B/-}$ P=0.0162).

Discussion

Gene therapy allows the modification of gene expression for therapeutic purposes, whereby gene addition involves the introduction of a functional transgene into the appropriate cells of the host. Therefore, the efficient delivery of therapeutic genes and appropriate gene expression systems are critical requirements for the development of an effective treatment (48). Benefits of an optimised system include significant reduction of vector dose needed to maintain transgene expression and lead to sufficient levels of protein production. Therefore, this study aimed to optimise a novel expression cassette for SMA, assessing integrative ability, promoters and transgene sequences for their effect on vector expression.

Our *in vitro* SMN restoration data provides similar results to those reported for existing lentiviral (49) and adenoviral (50) transduction as well as plasmid lipofection (51) and gene targeting (52). Limited use of lentiviral vectors for *in vivo* treatment of SMA has been reported, with the

early exception of Azzouz and colleagues (53). Here, we show evidence that a lentiviral expression system can efficiently restore SMN protein levels, especially when expressing our optimised transgene, *Co-hSMN1*. The four seminal papers that first demonstrated that viral vector-mediated expression of *SMN1 in vivo* on the day of birth provides amelioration of SMA phenotype, all used AAV vectors (54-57). Whilst these provided invaluable data and later led to the approval of Zolgensma as a licensed SMA therapy, it is also clear that no curative treatment is yet available for SMA. Our goal has been to develop a novel expression cassette, implemented in lentiviral vectors for cell culture testing and localised delivery *in vivo*, and in AAV vectors for widespread *in vivo* distribution.

Our optimisation has revealed that both IPLV and IDLV configurations encoding *SMN1* variants are efficient at transducing various *in vitro* models. Generally, IPLVs resulted in higher expression levels compared to their IDLV counterparts, although significant expression could still be obtained with the latter. The expression levels mediated by the IDLVs may actually be more adequate, as it has come to light that supraphysiological levels of SMN may be toxic (58), and IDLVs are a safer option without the potential risk of insertional mutagenesis from IPLVs. Transgenic expression levels of *SMN1* can also be controlled through the choice of promoter. Our *in vitro* experiments revealed that the ubiquitous CMV promoter directed the most robust transgene expression from lentiviral vectors. The strong and constitutive nature of this promoter lends itself to the systemic nature of SMA, as CMV can mediate gene expression in a remarkably broad range of cells. Intermediate transgenic expression levels were achieved with the ubiquitous hPGK promoter, while the neuron-specific hSYN promoter appeared the weakest of the three, despite the use of relevant neuronal systems as well as human fibroblasts.

Codon-optimisation of the *hSMN1* cDNA had a significant positive impact on the efficiency of the transgenic expression in all the cell culture systems evaluated. Implementation of the

optimised transgene in an AAV9 vector for *in vivo* delivery in *Smn*$^{2B/-}$ mice demonstrated robust expression in liver and spinal cord, at somewhat variable levels that on average were not significantly different from wild-type. Whilst the scope of the *in vivo* work presented here was limited to demonstrating effective transgenic expression, our cell culture experiments have shown dose-dependent expression from lentiviral vectors, which presumably could be replicated *in vivo* to titrate expression levels to an optimum. This is important, given the potential toxicity of SMN over-production (58).

The goal of maximizing correction of the SMA phenotype through the concurrent actions of several therapeutic compounds, or delivery routes, is gaining traction within the SMA field (59). Combinatorial delivery of a systemic AAV9 and a locally injected AAV or lentiviral vector to reinforce strong expression at specific locations might be a future avenue of investigation. A second possible strategy in which to use either AAV or lentiviral vectors expressing *SMN* would be *in utero* delivery. This has been attempted recently for SMA using AAV9 vectors and intracerebroventricular injections in mice fetuses. The results have shown encouraging rescue of the SMA phenotype but also significantly enhanced abortion rates of SMA mice compared to heterozygous or wild-type counterparts, pointing to potentially increased sensitivity to the procedure in SMA animals (60). Fetal delivery of IDLVs injected intraspinally has led to widespread expression of *eGFP* at all levels of the spinal cord in mice, underscoring the potential promise of this delivery system (61).

Several groups have found proteins associated with DNA damage and apoptosis to be dysregulated in SMA systems, including cleaved caspase 3 (41, 62), pATM , DNA-PKcs (43), senataxin (43), CHK2, pBRCA1, p53 (63) and γH2AX (63, 64). Signals indicative of genomic instability caused by DNA double strand breaks are transduced by ATM and downstream proteins including H2AX, leading to DNA repair by proteins such as BRCA1; or if damage is too

severe, apoptosis. Evidence of SMN restoration being able to revert some molecular signatures of the DNA damage response has been reported in the literature (40-43). In contrast, we found here that lentiviral transduction caused an increase in pATM levels, in the percentage of SMA fibroblasts that exhibited γH2AX foci as well as in the number of foci per cell, indicative of activation of the DNA damage response pathway. However, we did observe that the *Co-hSMN1* transgene had a protective effect in fibroblasts compared to *eGFP*-expressing vector regarding the induction of pATM.

A possible explanation for increase in γH2AX foci and pATM following IDLV transduction could be short-term initiation of host anti-viral responses which then activate the DNA damage response pathway. Lentiviral vector transduction is likely to trigger host anti-viral responses causing an increase in Toll-like receptor- (65) and type I interferon-signaling (66). Endocytosis of vectors, presence of the RNA:DNA hybrids following reverse transcription acting as a pathogen-associated molecular pattern, or plasmid contamination in laboratory-grade vector preparations could all alert the cell to presence of the viral vector (65). Finally, third generation lentiviral vectors lack pathogenic proteins such as Vpr, whose role normally is to counteract host anti-viral factors (65). Interferon-γ treatment has been shown to activate ATM (67), a process that involves autophosphorylation thus leading to increased pATM, like that seen here in SMA type I cells. Unrepaired DNA lesions, such as those evidenced by the increased γH2AX foci in SMA fibroblasts seen here, prime the type I interferon system leading to enhanced anti-viral responses upon encounter with viral particles (67, 68), potentially explaining why lentiviral vector transduction increased levels of γH2AX protein further. Following on from our work, further investigations are needed into both the benefits and potential detriments of viral transduction, specifically with regard to DNA damage and apoptotic protein expression changes following *in vivo* administration.

The outlook of therapy for SMA is continuing to look positive with three therapies licensed for clinical use, as well as an increasing number of other therapeutic strategies in the pipeline. Here, we have presented promising steps towards the development of a new strategy focused on delivery of a codon-optimised transgene, *Co-hSMN1*. Lentiviral-mediated expression of *Co-hSMN1* is able to rescue SMN expression in multiple *in vitro* cell systems and AAV9 delivery leads to strong expression in the *Smn*$^{2B/-}$ mouse model of SMA. Future experimentation should continue to explore long-term benefits of this therapeutic strategy on survival and motor performance of SMA mice, whilst also delving into any unexpected genotoxic consequences of viral transduction.

Author contributions

EMC and NAMN performed *in vitro* experimentation and analyses. MB performed *in vivo* injections and tissue harvests whilst SO analysed tissue from *in vivo* experiments. HF provided support for animal experimentation. RJY-M provided conceptual support and interpretation of results. All authors contributed to manuscript preparation.

Competing interests

NAMN, EMC and RJY-M have filed a patent application on the uses of the novel SMN transgene reported in this manuscript. SB, HRF and MB report no conflicts of interest.

Funding

EMC was partially funded by a scholarship from Royal Holloway University of London. NAMN was partially funded by a scholarship and student stipend, from Royal Holloway University of London and The Spinal Muscular Atrophy Trust. HF acknowledges financial support for SMA research from the Great Ormond Street Hospital Charity (GOSH) which funds SO (Grant No.

V5018). RJY-M acknowledges general financial support from SMA UK (formerly The SMA Trust), through the UK SMA Research Consortium, for SMA research in his laboratory. MB acknowledges general financial support from SMA UK, Muscular Dystrophy UK, Action Medical Research, SMA Angels Charity and Academy of Medical Sciences for SMA research in her laboratory.

References

1. Lefebvre S, Burgen L, Reboullet S, Clermont O, Burlet P, Viollet L, et al. Identification and characterisation of a spinal muscular atrophy-determining gene. Cell. 1995;80(155-165).
2. Lorson CL, Hahnen E, Androphy EJ, Wirth B. A single nucleotide in the SMN gene regulates splicing and is responsible for spinal muscular atrophy. Proc Natl Acad Sci U S A. 1999;96(11):6307-11.
3. Monani UR, Lorson CL, Parsons DW, Prior TW, Androphy EJ, Burghes AHM, et al. A single nucleotide difference that alters splicing patterns distinguishes the SMA gene SMN1 from the copy gene SMN2. Human Molecular Genetics. 1999;8(7):1177-83.
4. Butchbach MER. Copy Number Variations in the Survival Motor Neuron Genes: Implications for Spinal Muscular Atrophy and Other Neurodegenerative Diseases. Frontiers in Molecular Biosciences. 2016;3.
5. Harada Y, Sutomo R, Sadewa A, Akutsu T, Takeshima Y, Wada H, et al. Correlation between SMN2 copy number and clinical phenotype of spinal muscular atrophy: three SMN2 copies fail to rescue some patients from the disease severity. J Neurol. 2002;249:1211-9.
6. Calucho M BS, Alías L, March F, Venceslá A, Rodríguez-Álvarez FJ, Aller E, Fernández RM, Borrego S, Millán JM, Hernández-Chico C, Cuscó I, Fuentes-Prior P, Tizzano EF. . Correlation between SMA type and SMN2 copy number revisited: An analysis of 625 unrelated Spanish patients and a compilation of 2834 reported cases. . Neuromuscul Disord 2018;28(3):208-15.
7. Singh RN, Howell MD, Ottesen EW, Singh NN. Diverse role of survival motor neuron protein. Biochemica et Biophysica Acta. 2017;1860:299-315.
8. Gavrilina TO, McGovern VL, Workman E, Crawford TO, Gogliotti RG, DiDonato CJ, et al. Neuronal SMN expression corrects spinal muscular atrophy in severe SMA mice while muscle-specific SMN expression has no phenotypic effect. Human Molecular Genetics. 2008;17:1063-75.
9. Hamilton G, Gillingwater TH. Spinal muscular atrophy: going beyond the motor neuron. Trends in Molecular Medicine. 2013;19(1):40-50.
10. Singh NK, Singh NN, Androphy EJ, Singh RN. Splicing of a critical exon of human survival motor neuron is regulated by a unique silencer element located in the last intron. Molecular and Cellular Biology. 2006;26(4):1333-46.
11. Singh NN, Howell MD, Androphy EJ, Singh RN. How the discovery of ISS-N1 led to the first medical therapy for spinal muscular atrophy. Gene Therapy. 2017;24(9):520-6.

12. Mendell JR, Al-Zaidy S, Shell R, Arnold WD, Rodino-Klapac LR, Prior TW, et al. Single-Dose Gene-Replacement Therapy for Spinal Muscular Atrophy. New England Journal of Medicine. 2017;377(18):1713-22.
13. Baranello G, Darras BT, Day JW, Deconinck N, Klein A, Masson R, et al. Risdiplam in Type 1 Spinal Muscular Atrophy. New England Journal of Medicine. 2021;384(10):915-23.
14. Blömer U, Naldini L, Kafri T, Trono D, Verma IM, Gage FH. Highly efficient and sustained gene transfer in adult neurons with a lentivirus vector. . Journal of Virology. 1997;71:6641–9.
15. Frankel D, Young J. HIV-1: fifteen proteins and an RNA. . Annual Review of Biochemistry. 1998;67:1–25.
16. Picanco-Castro V, de Sousa Russo-Carbolante EM, Tadeu Covas D. Advances in lentiviral vectors: a patent review. Recent Patents on DNA & Gene Sequences. 2012;6:82–90.
17. Vigna E, Naldini L. Lentiviral vectors: excellent tools for experimental gene transfer and promising candidates for gene therapy. Journal of Gene Medicine. 2000;2(5):308-16.
18. Throm RE, Ouma AA, Zhou S, Chandrasekaran A, Lockey T, Greene M, et al. Efficient construction of producer cell lines for a SIN lentiviral vector for SCID-X1 gene therapy by concatemeric array transfection. Blood. 2009;113:5104–10.
19. Zhao H, Pestina TI, Nasimuzzaman M, Mehta P, Hargrove PW, Persons DA. Amelioration of murine beta-thalassemia through drug selection of hematopoietic stem cells transduced with a lentiviral vector encoding both gamma-globin and the MGMT drug-resistance gene. Blood. 2009;113:5747–56.
20. Mantovani J, Charrier S, Eckenberg R, Saurin W, Danos O, Perea J, et al. Diverse genomic integration of a lentiviral vector developed for the treatment of Wiskott-Aldrich syndrome. The Journal of Gene Medicine. 2009;11:645–
54.
21. Biffi A, Naldini L. Novel candidate disease for gene therapy: metachromatic leukodystrophy. Expert Opinion on Biological Therapy. 2007;7:1193– 205.
22. Brown BD, Cantore A, Annoni A, Sergi LS, Lombardo A, Della Valle P, et al. A microRNA-regulated lentiviral vector mediates stable correction of hemophilia B mice. Blood. 2007;110:4144–52.
23. Jacome A, Navarro S, Río P, Yañez RM, González-Murillo A, Lozano ML, et al. Lentiviral-mediated genetic correction of hematopoietic and mesenchymal progenitor cells from Fanconi anemia patients. . Molecular Therapy. 2009;17:1083–92.
24. Menzel O, Birraux J, Wildhaber BE, Jond C, Lasne F, Habre W, et al. Biosafety in ex vivo gene therapy and conditional ablation of lentivirally transduced hepatocytes in nonhuman primates. Molecular Therapy. 2009;17:1754–60.
25. Schuster SJ, Bishop, M. R., Tam, C. S., Waller, E. K., Borchmann, P., Mcguirk, J. P., et al. Primary analysis of juliet: a global, pivotal, phase 2 Trial of CTL019 in adult patients with relapsed or refractory diffuse large B-cell lymphoma. . Blood. 2017;130:577-.
26. Maude SL, Laetsch, T. W., Buechner, J., Rives, S., Boyer, M., Bittencourt, H., et al. Tisagenlecleucel in Children and Young Adults with B-Cell Lymphoblastic Leukemia. . New England Journal of Medicine. 2018;378:439–48.
27. Thompson AA, Walters MC, Kwiatkowski J, Rasko JEJ, Ribeil J-A, Hongeng S, et al. Gene Therapy in Patients with Transfusion-Dependent β-Thalassemia. New England Journal of Medicine. 2018;378(16):1479-93.
28. Hacein-Bey-Abina S, Von Kalle C, Schmidt M, McCcormack MP, Wulffraat N, Leboulch P, et al. LMO2-associated clonal T cell proliferation in two patients after gene therapy for SCID-X1. Science. 2003;302(5644):415-9.
29. Gaspar HB, Parsley KL, Howe S, King D, Gilmour KC, Sinclair J, et al. Gene therapy of X-linked severe combined immunodeficiency by use of a pseudotyped gammaretroviral vector. Lancet. 2004;364(9452):2181-7.

30. Howe SJ, Mansour MR, Schwarzwaelder K, Bartholomae C, Hubank M, Kempski H, et al. Insertional mutagenesis combined with acquired somatic mutations causes leukemogenesis following gene therapy of SCID-X1 patients. Journal of Clinical Investigation. 2008;118(9):3143-50.
31. Yáñez-Muñoz RJ, Balaggan KS, MacNeil A, Howe SJ, Schmidt M, Smith AJ, et al. Effective gene therapy with nonintegrating lentiviral vectors. Nature Medicine. 2006;12(3):348-53.
32. Bowerman M, Murray LM, Beauvais A, Pinheiro B, Kothary R. A critical smn threshold in mice dictates onset of an intermediate spinal muscular atrophy phenotype associated with a distinct neuromuscular junction pathology. Neuromuscular Disorders. 2012;22(3):263-76.
33. Boza-Moran MG, Martinez-Hernandez R, Bernal S, Wanisch K, Also-Rallo E, Le Heron A, et al. Decay in survival motor neuron and plastin 3 levels during differentiation of iPSC-derived human motor neurons. Scientific Reports. 2015;5:11696.
34. Lu-Nguyen NB, Broadstock M, Yáñez-Muñoz RJ. Efficient expression of Igf-1 from lentiviral vectors protects in vitro but does not mediate behavioral recovery of a Parkinsonian lesion in rats. Human Gene Therapy. 2015;26:719-33.
35. Peluffo H, Foster E, Ahmed SG, Lago N, Hutson TH, Moon L, et al. Efficient gene expression from integration-deficient lentiviral vectors in the spinal cord. Gene Ther. 2013;20(6):645-57.
36. Maury Y, Come J, Piskorowski RA, Salah-Mohellibi N, Chevaleyre V, Peschanski M, et al. Combinatorial analysis of developmental cues efficiently converts human pluripotent stem cells into multiple neuronal subtypes. Nature Biotechnol. 2015;33(1):89-96.
37. Šoltić D, Bowerman M, Stock J, Shorrock HK, Gillingwater TH, H.R. F. Multi-Study Proteomic and Bioinformatic Identification of Molecular Overlap between Amyotrophic Lateral Sclerosis (ALS) and Spinal Muscular Atrophy (SMA). Brain Sciences. 2018;8(212).
38. Young PJ, Le TT, Thi Man N, Burghes AHM, Morris GE. The relationship between SMN, the spinal muscular atrophy protein, and nuclear coiled bodies in differentiated tissues and cultured cells. Exp Cell Res. 2000;256:365-74.
39. Abràmoff MD, Magalhães PJ, Ram SJ. Image processing with imageJ. . Biophotonics Int. 2004;11:36-41.
40. Vyas S, Bechade C, Riveau B, Downward J, Triller A. Involvement of survival motor neuron (SMN) protein in cell death. Human Molecular Genetics. 2002;11(22):2751-64.
41. Parker GC, Li XL, Anguelov RA, Toth G, Cristescu A, Acsadi G. Survival motor neuron protein regulates apoptosis in an in vitro model of spinal muscular atrophy. Neurotoxicity Research. 2008;13(1):39-48.
42. Young PJ, Day PM, Zhou J, Androphy EJ, Morris GE, Lorson CL. A direct interaction between the survival motor neuron protein and p53 and its relationship to spinal muscular atrophy. Journal of Biological Chemistry. 2002;277(4):2852-9.
43. Kannan A, Bhatia K, Branzei D, Gangwani L. Combined deficiency of Senataxin and DNA-PKcs causes DNA damage accumulation and neurodegeneration in spinal muscular atrophy. Nucleic Acids Research. 2018;46(16):8326-46.
44. Rogakou EP, Pilch DR, Orr AH, Ivanova VS, Bonner WM. DNA double-stranded breaks induce histone H2AX phosphorylation on serine 139. Journal of Biological Chemistry. 1998;273(10):5858-68.
45. Rogakou EP, Boon C, Redon C, Bonner WM. Megabase chromatin domains involved in DNA double-strand breaks in vivo. Journal of Cell Biology. 1999;146(5):905-15.
46. Martin SJ, Green DR. Protease activation during apoptosis: death by a thousand cuts? Cell. 1995;82(3):349-52.
47. Blackford AN, Jackson SP. ATM, ATR, and DNA-PK: The Trinity at the Heart of the DNA Damage Response. Mol Cell. 2017;66(6):801-17.

48. Walther W, Stein U. Viral vectors for gene transfer: a review of their use in the treatment of human diseases. Drugs. 2000;60:249–71.
49. Valori CF, Ning K, Wyles M, Mead RJ, Grierson AJ, Shaw PJ, et al. Systemic delivery of scAAV9 expressing SMN prolongs survival in a model of spinal muscular atrophy. Science Translational Medicine. 2010;2(35):35ra42.
50. DiDonato CJ, Parks RJ, Kothary R. Development of a gene therapy strategy for the restoration of survival motor neuron protein expression: implications for spinal muscular atrophy therapy. Human Gene Therapy. 2003;14(2):179-88.
51. Rashnonejad A, Chermahini GA, Li SY, Ozkinay F, Gao GP. Large-Scale Production of Adeno-Associated Viral Vector Serotype-9 Carrying the Human Survival Motor Neuron Gene. Molecular Biotechnology. 2016;58(1):30-6.
52. Feng M, Liu C, Xia Y, Liu B, Zhou M, Li Z, et al. Restoration of SMN expression in mesenchymal stem cells derived from gene-targeted patient-specific iPSCs. Journal of Molecular Histology. 2018;49:27-37.
53. Azzouz M, Le T, Ralph GS, Walmsley L, Monani UR, Lee DC, et al. Lentivector-mediated SMN replacement in a mouse model of spinal muscular atrophy. Journal of Clinical Investigation. 2004;114(12):1726-31.
54. Foust KD, Wang XY, McGovern VL, Braun L, Bevan AK, Haidet AM, et al. Rescue of the spinal muscular atrophy phenotype in a mouse model by early postnatal delivery of SMN. Nature Biotechnology. 2010;28(3):271-U126.
55. Passini MA, Bu J, Roskelley EM, Richards AM, Sardi SP, O'Riordan CR, et al. CNS-targeted gene therapy improves survival and motor function in a mouse model of spinal muscular atrophy. J Clin Invest. 2010;120(4):1253-64.
56. Valori CF, Ning K, Wyles M, Mead RJ, Grierson AJ, Shaw PJ, et al. Systemic delivery of scAAV9 expressing SMN prolongs survival in a model of spinal muscular atrophy. Sci Transl Med. 2010;2(35):35ra42.
57. Dominguez E, Marais T, Chatauret N, Benkhelifa-Ziyyat S, Duque S, Ravassard P, et al. Intravenous scAAV9 delivery of a codon-optimized SMN1 sequence rescues SMA mice. Hum Mol Genet. 2011;20(4):681-93.
58. Van Alstyne M, Tattoli I, Delestree N, Recinos Y, Workman E, Shihabuddin LS, et al. Gain of toxic function by long-term AAV9-mediated SMN overexpression in the sensorimotor circuit. Nature Neuroscience. 2021;24(7):930-+.
59. Bowerman M, Becker CG, Yáñez-Muñoz RJ, Ning K, Wood M, Gillingwater TH, et al. Therapeutic strategies for spinal muscular atrophy: SMN and beyond. Disease Models & Mechanisms. 2017;10:943-54.
60. Rashnonejad A, Chermahini GA, Gunduz C, Onay H, Aykut A, Durmaz B, et al. Fetal Gene Therapy Using a Single Injection of Recombinant AAV9 Rescued SMA Phenotype in Mice. Molecular Therapy. 2019;27(12):2123-33.
61. Ahmed SG, Waddington SN, Boza-Moran MG, Yáñez-Muñoz RJ. High-efficiency transduction of spinal cord motor neurons by intrauterine delivery of integration-deficient lentiviral vectors. Journal of Controlled Release. 2018;273:99-107.
62. Sareen D, Ebert AD, Heins BM, Mcgivern JV, Ornelas L, Svendsen CN. Inhibition of Apoptosis Blocks Human Motor Neuron Cell Death in a Stem Cell Model of Spinal Muscular Atrophy. . Plos One. 2012;7.
63. Jangi M, Fleet C, Cullen P, Gupta SV, Mekhoubad S, Chiao E, et al. SMN deficiency in severe models of spinal muscular atrophy causes widespread intron retention and DNA damage. Proc Natl Acad Sci U S A. 2017;114(12):E2347-E56.
64. Mutsaers CA, Wishart, T.M., Lamont, D.J., Riessland, M., Schreml, J., Comley, L.H., Murray, L.M., Parson, S.H., Lochmuller, H., Wirth, B., Talbot, K., Gillingwater, T.H. . Reversible molecular pathology of skeletal muscle in spinal muscular atrophy. . Human Molecular Genetics. 2011;20:4334-44.

65. Kajaste-Rudnitski A, Naldini L. Cellular Innate Immunity and Restriction of Viral Infection: Implications for Lentiviral Gene Therapy in Human Hematopoietic Cells. Human Gene Therapy. 2015;26(4):201-9.
66. Maillard PV, van der Veen AG, Poirier EZ, Reis e Sousa C. Slicing and dicing viruses: antiviral RNA interference in mammals. Embo Journal. 2019;38(8).
67. Morales AJ, Carrero JA, Hung PJ, Tubbs AT, Andrews JM, Edelson BT, et al. A type I IFN-dependent DNA damage response regulates the genetic program and inflammasome activation in macrophages. Elife. 2017;6.
68. Hartlova A, Erttmann SF, Raffi FAM, Schmalz AM, Resch U, Anugula S, et al. DNA Damage Primes the Type I Interferon System via the Cytosolic DNA Sensor STING to Promote Anti-Microbial Innate Immunity. Immunity. 2015;42(2):332-43.

Figure legends

Figure 1: Maps displaying features of the transfer plasmids encoding *Co-hSMN1* or control *eGFP*.

The constructs used in transfer plasmids to produce (A-D) lentiviral or (E,F) adeno-associated viral (AAV) vectors are shown. Each plasmid encodes the *Co-hSMN1* or *eGFP* transgene flanked upstream by a promoter (CMV, hSYN, hPGK or chicken beta-actin CMV hybrid (CAG)) and downstream by woodchuck hepatitis post-transcriptional regulatory element (WPRE; mutated in constructs A-C and E), a post-transcriptional element that improves transgene expression (except in the case of AAV_CAG_*eGFP* (F)).

Figure 2: Lentiviral vector-mediated *hSMN1* and *Co-hSMN1* expression in mouse primary cortical neurons and rat primary motor neurons.

3-week old mouse primary cortical cultures and isolated motor neuron cultures from E15 rat embryos were transduced with IPLVs and IDLVs encoding CMV_*hSMN1,* CMV_*Co-hSMN1,* hSYN_*hSMN1* or hSYN_*Co-hSMN1* cassettes, with cells collected at 72h post-transduction. (A) qPCR MOI 30 and 100 were used to transduce mouse cortical neuronal cultures, which were analysed by western blot and SMN protein levels were quantified in (B). Representative western

747 blots are shown and statistical comparisons can be found in Table S1. (C) Motor neurons were
748 transduced at qPCR MOI 30, 60 or 100. Immunofluorescence images show examples of
749 transduced cells at MOI 60, 72h post-transduction. Scale bars = 20 μm. (D) Quantification of
750 SMN immunofluorescence in cell bodies of transduced or control E14 rat primary motor
751 neurons. Statistical comparisons can be found in Table S2. Error bars represent standard
752 deviation. N=3 biological replicates were collected in each case.
753
754 **Figure 3: Assessment of SMN protein levels in iPSC motor neurons.** (A) Representative
755 images of mature, SMA type I iPSC-derived motor neurons at both high and low seeding
756 density. Scale bar = 100 μm (high density, top image) and 50 μm (low density, bottom image).
757 (B) Immunofluorescence images of control and IDLV_CMV_*Co-hSMN1*-transduced SMA type I
758 iPSC motor neurons. Scale bar = 20 μm (top image) and 50 μm (bottom image). (C)
759 Representative western blots showing total protein (red) and SMN (green) in triplicate samples
760 from three independent SMA type I iPSC MN lines mock-transduced or transduced with IDLVs
761 expressing *Co-hSMN1* under transcriptional control of CMV, hSYN or hPGK promoters. (D)
762 Quantification of western blots. Error bars represent standard deviation. No significant
763 difference was seen between the three untransduced wild type lines, or between the three SMA
764 type I lines. Significance represented by stars on transduced samples indicates a comparison to
765 the control SMN levels in that particular line. * P<0.05, ** P<0.01, *** P<0.001, **** P<0.0001.
766 N=3 biological replicates were collected for each line, as well as three independent lines for
767 each genotype used.
768
769 **Figure 4: SMN levels in primary SMA type I patient fibroblasts following IDLV**
770 **transduction.**
771 (A) Representative immunofluorescent images of wild-type and SMA type I fibroblasts after
772 IDLV_CMV_*Co-hSMN1* transduction at qPCR MOI 75 and 100, plus control. Scale bars = 50

773 μm in all images. (B) Western blots from cells harvested 72h post-transduction with IDLVs at
774 MOI 75 and 100. (C) Quantification of western blots. Error bars represent standard deviation. *
775 P<0.05, ** P<0.01, *** P<0.001, **** P<0.0001. N=3 biological replicates were collected in each
776 case.
777
778 **Figure 5: Restoration of gems in SMA type I fibroblasts transduced with lentiviral vectors**
779 **encoding *hSMN1* or *Co-hSMN1*.**
780 Cultured human SMA type I fibroblasts were transduced with IPLVs or IDLVs encoding
781 CMV_*hSMN1,* CMV_*Co-hSMN1,* hSYN_*hSMN1* or hSYN_*Co-hSMN1* cassettes at qPCR MOI
782 30, 60 or 100. The number of gems present in 100 nuclei was quantified 72h post-transduction.
783 (A) Representative images of gems in control human fibroblasts, non-transduced and SMA type
784 I cells transduced at MOI 100. Statistical comparisons can be found in Table S3. Scale bars = 5
785 μm. (B) Quantification of (A). Error bars represent standard deviation. N=3 biological replicates
786 were collected in each case.
787
788 **Figure 6: The effect of IDLV_CMV_*Co-hSMN1* transduction on γH2AX foci in SMA type I**
789 **fibroblasts.**
790 (A) SMA type I fibroblasts were immunostained for γH2AX 72h post-transduction with
791 IDLV_CMV_*Co-hSMN1* at MOI 75. Scale bars = 20 μm in images of wild-type and SMA type I
792 cells, and 50 μm in transduced cells. A view of cells of interest (white dotted line) at increased
793 magnification (lower panel) shows nuclear foci more clearly. (B) The number of foci per cell and
794 (C) percentage of foci-positive cells were quantified. Error bars represent standard deviation. *
795 P<0.05, ** P<0.01. N=3 biological replicates were collected in each case with each technical
796 replicate quantifying at least n=25 cells.
797

Figure 7: ATM and pATM in wild-type and SMA type I fibroblasts and SMA type I iPSC-derived motor neurons.

Quantification of western blots using protein lysates from wild-type, SMA type I fibroblasts and SMA type I fibroblasts treated with 200 μM hydrogen peroxide (H_2O_2) for 2 hours prior to lysis assessing (A) ATM and (B) pATM levels. (C) Transduction of SMA type I fibroblasts with either IDLV_CMV_*eGFP* or IDLV_CMV_*Co-hSMN1* (both MOI 75) for either 3 or 7 days before harvest and pATM western blot. (D,E) Quantification of ATM and pATM western blots from three independent lines of SMA type I iPSC-derived motor neurons transduced at maturity with IDLV_CMV_*Co-hSMN1* (MOI 75) and harvested 3 days post-transduction. Error bars represent standard deviation. * P<0.05, ** P<0.01, *** P<0.001, **** P<0.0001. N=3 biological replicates were collected in each case. See Supplementary Figure 4 for representative western blot images.

Figure 8: Analysis of SMN levels following *in vivo* neonatal administration of AAV9 vectors expressing *Co-hSMN1.*

Smn$^{2B/-}$ neonatal (P0) mice were administered AAV9_CAG_*eGFP* or AAV9_CAG_*Co-hSMN1* and their livers (A,B) and spinal cords (C,D) harvested at the symptomatic time-point of P18 for protein analysis. SMN protein levels were normalised to those in wild-type samples in all cases. Error bars represent standard deviation. * P<0.05, ** P<0.01. Wild-type n=4, untreated *Smn*$^{2B/-}$ n=3, *Smn*$^{2B/-}$ + AAV9_CAG_*eGFP* n=5, *Smn*$^{2B/-}$ + AAV9_CAG_*Co-hSMN1* n=5 biological replicates.

Supplementary Figure 1: Pairwise alignment of wild-type and *Co-hSMN1* cDNA sequences.

The sequences of the wild-type *SMN1* cDNA (top) and the *Co-hSMN1* cDNA (bottom) open reading frames were aligned, and nucleotide differences highlighted with asterisks.

Supplementary Figure 2: Characterisation of cortical and motor neurons in culture.

(A) 6 day-old mouse cortical neuron cultures were fixed and stained with neuron marker (NeuN). Nuclei were stained blue with DAPI. (B) 72-hours post-seeding, rat motor neurons were fixed and immunostained for a common motor neuronal marker (ChAT) to confirm motor neuron identity. Scale bars = 100 μm.

Supplementary Figure 3: Characterisation of iPSC-derived motor neurons.

Representative images of motor neuron cells at different stages of the differentiation protocol. (A) OLIG2-positive (green) motor neuron progenitors at day 16 of differentiation. (B-D) Mature motor neurons express (B) SMI-32 (red) and βIII-tubulin (green), (C) HB9 (red) and (D) ChAT (green). All counterstained with DAPI (blue).

Supplementary Figure 4: Determining *SMN* transcript origin and SMN protein levels in iPSC-derived MNs.

An RT-PCR was performed using primers to amplify a region between exons 6-8 of the *SMN* genes in iPSC-derived MNs. -RT = minus reverse transcriptase control reaction. (A) Full length *SMN* (*FL-SMN*) products (504bp) and *SMNΔ7* transcripts (450bp) are shown. (B) Two control gene products (GAPDH: 184bp and β-actin: 295bp) were also amplified. The same lane order is present in all gels. (C) The two bands seen at 504 and 450bp in (A) were excised separately and purified. PCR amplicons were digested with *Dde*I for 2 hours before running digested products on a second gel to reveal diagnostic *Dde*I restriction site present only in *SMN2* transcripts. Cleavage products: *FL-SMN2* (504bp) = 382 and 122bp, *SMN2Δ7* (450bp) = 328 and 122bp. (D,E) SMA type I MNs show 18-fold ($P<0.0001$) less SMN protein than wild type MNs at day 31 of differentiation. N=3 biological replicates were collected for each line.

Supplementary Figure 5: Representative western blot images of ATM and pATM levels in SMA type I fibroblasts (top and middle panels) and iPSC-derived motor neurons (bottom panel).

Quantification can be found in Figure 7.

Supplementary Figure 6: Immunofluorescence staining pattern of cleaved caspase 3 and γH2AX in wild-type, SMA type I fibroblasts and SMA type I fibroblasts transduced with IDLV_CMV_*Co-hSMN1.*

Fibroblasts were immunostained against cleaved caspase 3 before the staining pattern was quantified. (A) A scoring system was designed to delineate levels of expression: 0 = no signal, 1 = less than 5 foci, 2 = more than 5 foci, 3 = light, diffuse staining, 4 = strong, diffuse staining throughout whole nucleus, or very strong expression in a concentrated area. Examples of nuclei representative of scores 1-4 are shown. (B) Values for each cleaved caspase 3 score as a percentage of total cells in each replicate were calculated and an unpaired, one-tailed t-test between wild-type and SMA (average 19 and 37 cells per replicate, respectively), at each score was conducted (0: P=0.0006, 1: P=0.0472, 2: P=0.0451, 3: P=0.4565, 4: P=0.1613). (C) The percentage of total SMA type I cells exhibiting each score was calculated, but large variation is seen in both mock and transduced samples. At least 30 cells per replicate were scored for each condition (total n=107 mock transduced cells, n=115 transduced cells). Significance was assessed at each score by unpaired, two-tailed t-tests (0: P=0.1751, 1: P=0.8194, 2: P=0.9031, 3: P=0.5228, 4: P=0.8709).

Supplementary Table 1: Comparison of SMN protein production from all vectors in primary mouse cortical neurons.

One-way ANOVA and Bonferroni's post-hoc test were used to determine significant differences in western data from transduced mouse cortical neurons (shown in Figure 2A-B). The data compare types of vectors, transgenes and promoters on protein production. Additionally, data were analysed to determine whether there was a dose-dependent increase within each group. Values represent mean ± SEM. * P<0.05, ** P<0.01, *** P<0.001. N=3 biological replicates were collected in each case.

Supplementary Table 2: Comparison of SMN protein production from all vectors in primary rat motor neurons.

One-way ANOVA and Bonferroni's post-hoc test were used to determine significant differences in immunofluorescence data from transduced primary rat motor neurons (shown in Figure 2C-D). Data compare types of vectors, transgenes and promoters on protein production. Additionally, data were analysed to determine whether there was a dose-dependent increase within each group. Values represent mean ± SEM. * P<0.05, ** P<0.01, *** P<0.001. N=3 biological replicates were collected in each case.

Supplementary Table 3: Comparison of gem restoration by all vectors in SMA type I fibroblasts.

One-way ANOVA and Bonferroni's post-hoc test was used to determine significant differences in type I SMA fibroblast populations (shown in Figure 5). The analysed data show the effect of different parameters such as lentiviral vector configuration, transgene and promoter, on gem restoration. In addition, data were analysed to determine whether there were dose-dependent increases within each promoter group. Values represent mean ± SEM. * P<0.05, ** P<0.01, *** P<0.001. N=3 biological replicates were collected in each case.

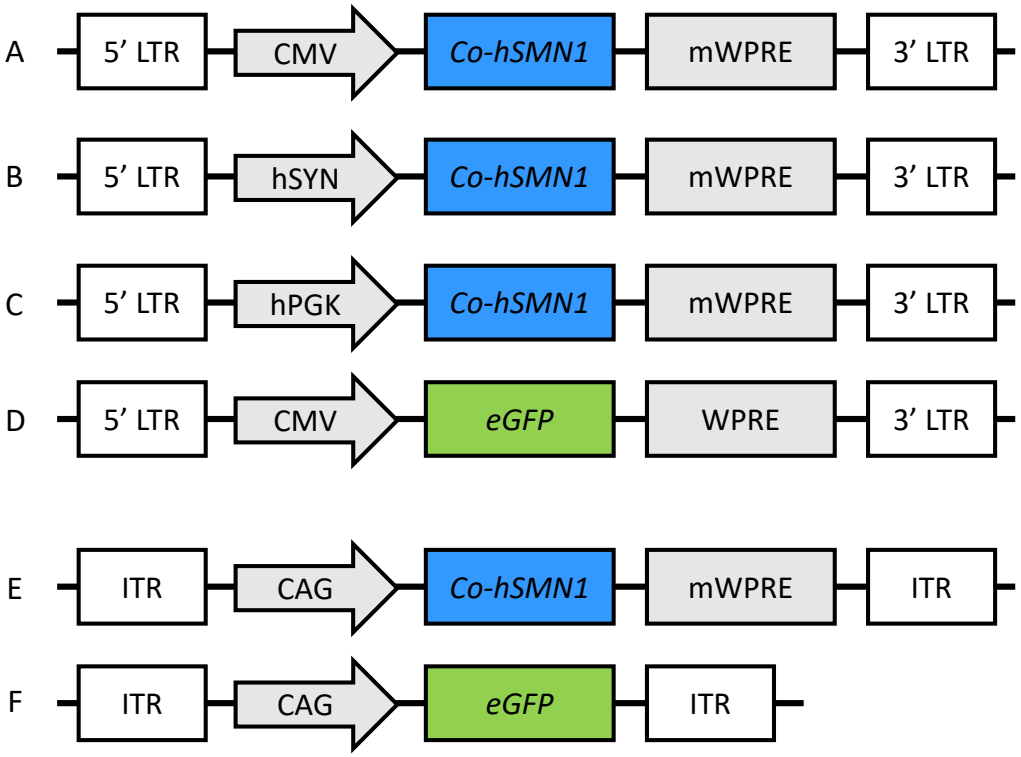
A
5’ LTR
CMV
Co-hSMN1
mWPRE
3’ LTR
B
5’ LTR
hSYN
Co-hSMN1
mWPRE
3’ LTR
C
5’ LTR
hPGK
Co-hSMN1
mWPRE
3’ LTR
D
5’ LTR
CMV
eGFP
WPRE
3’ LTR
E
ITR
CAG
Co-hSMN1
mWPRE
ITR
F
ITR
CAG
eGFP
ITR

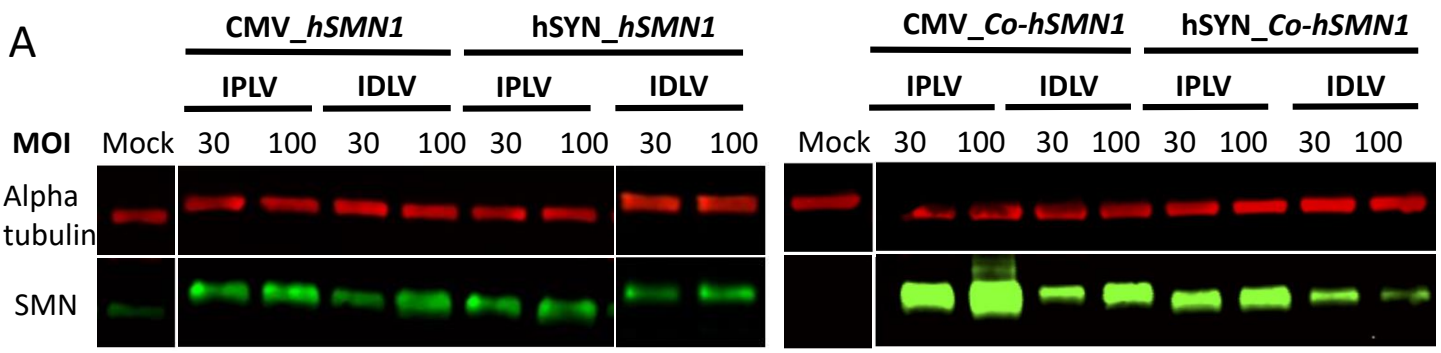
A
CMV_hSMN1
hSYN_hSMN1
CMV_Co-hSMN1
hSYN_Co-hSMN1
IPLV
IDLV
IPLV
IDLV
IPLV
IDLV
MOI
Mock
30
100
30
100
30
100
30
100
Mock
30
100
30
100
30
100
30
100
Alpha tubulin
SMN

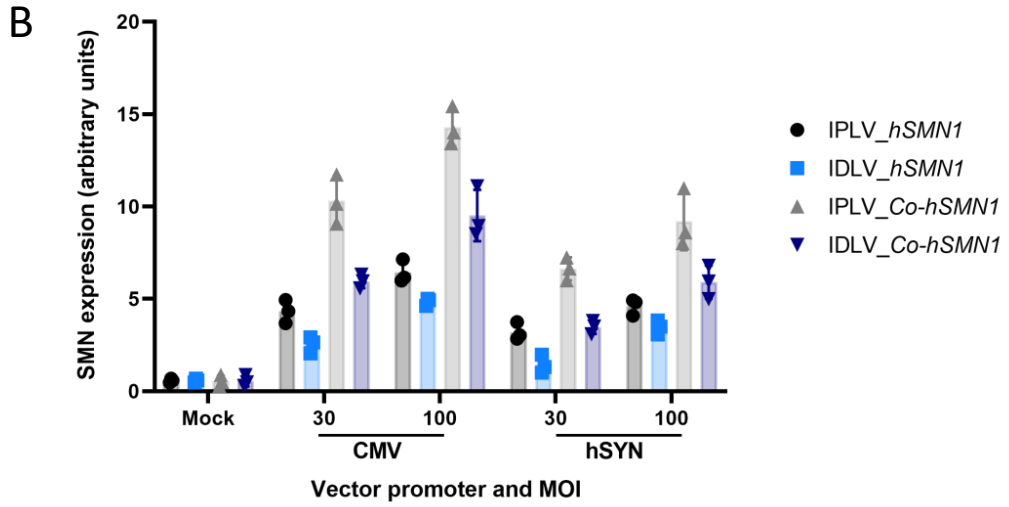
B
SMN expression (arbitrary units)
20
15
10
5
0
Mock
30
100
30
100
CMV
hSYN
Vector promoter and MOI
IPLV_hSMN1
IDLV_hSMN1
IPLV_Co-hSMN1
IDLV_Co-hSMN1

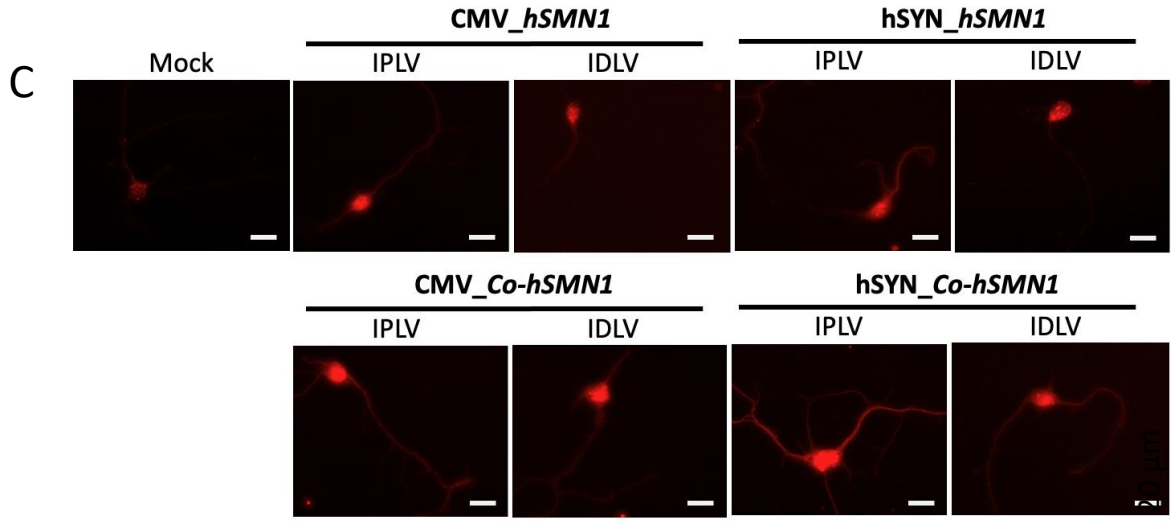
C
Mock
CMV_hSMN1
hSYN_hSMN1
IPLV
IDLV
IPLV
IDLV
CMV_Co-hSMN1
hSYN_Co-hSMN1
IPLV
IDLV
IPLV
IDLV

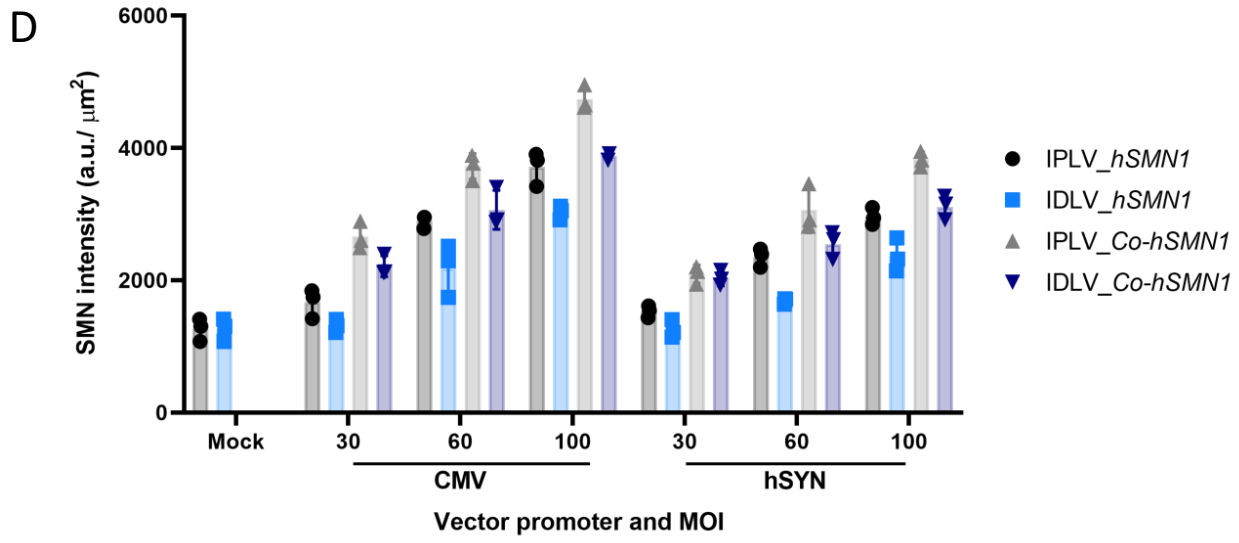
D
SMN intensity (a.u./ μm²)
6000
4000
2000
0
Mock
30
60
100
30
60
100
CMV
hSYN
Vector promoter and MOI
IPLV_hSMN1
IDLV_hSMN1
IPLV_Co-hSMN1
IDLV_Co-hSMN1

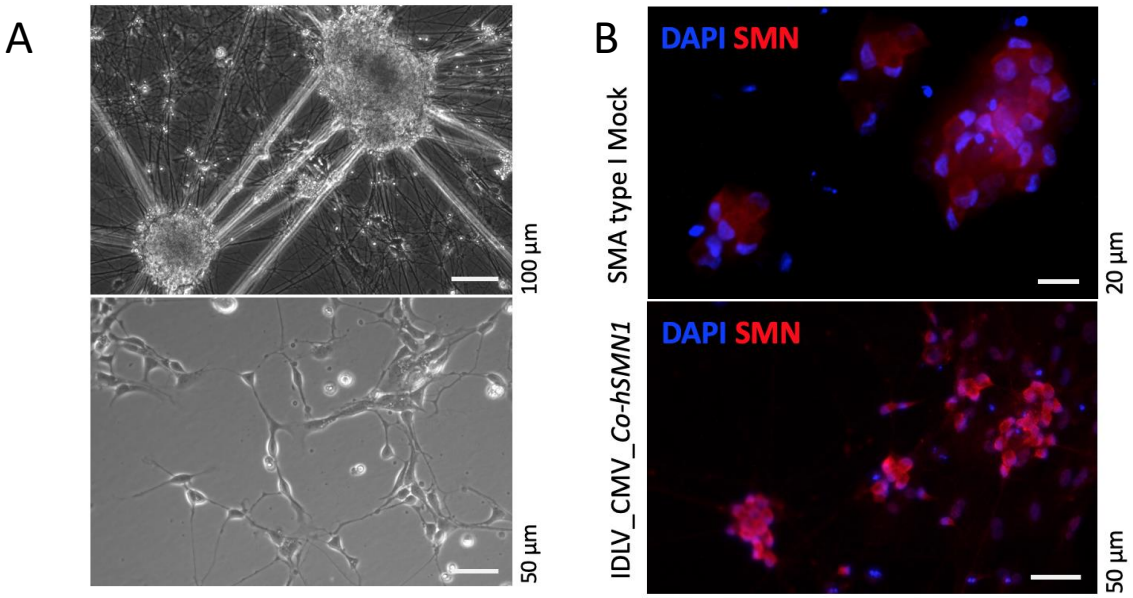
A
100 µm
50 µm
B
DAPI SMN
SMA type I Mock
IDLV_CMV_Co-hSMN1
20 µm
50 µm

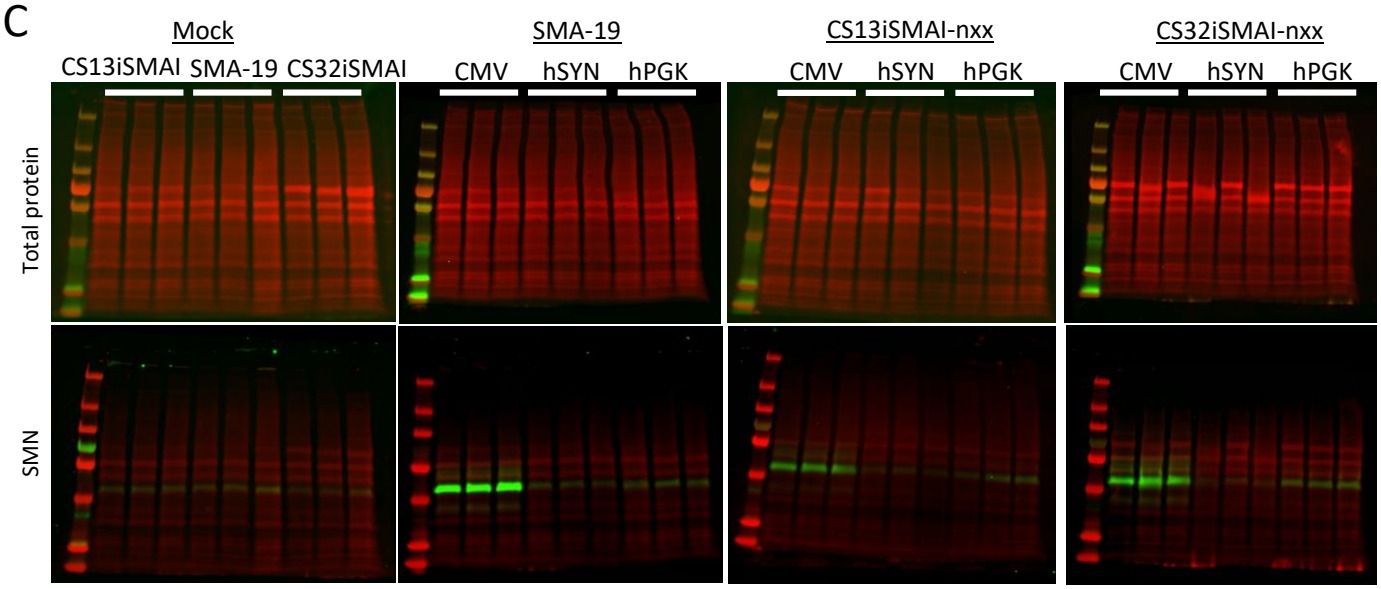
C
Mock
SMA-19
CS13iSMAI-nxx
CS32iSMAI-nxx
CS13iSMAI SMA-19 CS32iSMAI
CMV hSYN hPGK
CMV hSYN hPGK
CMV hSYN hPGK
Total protein
SMN

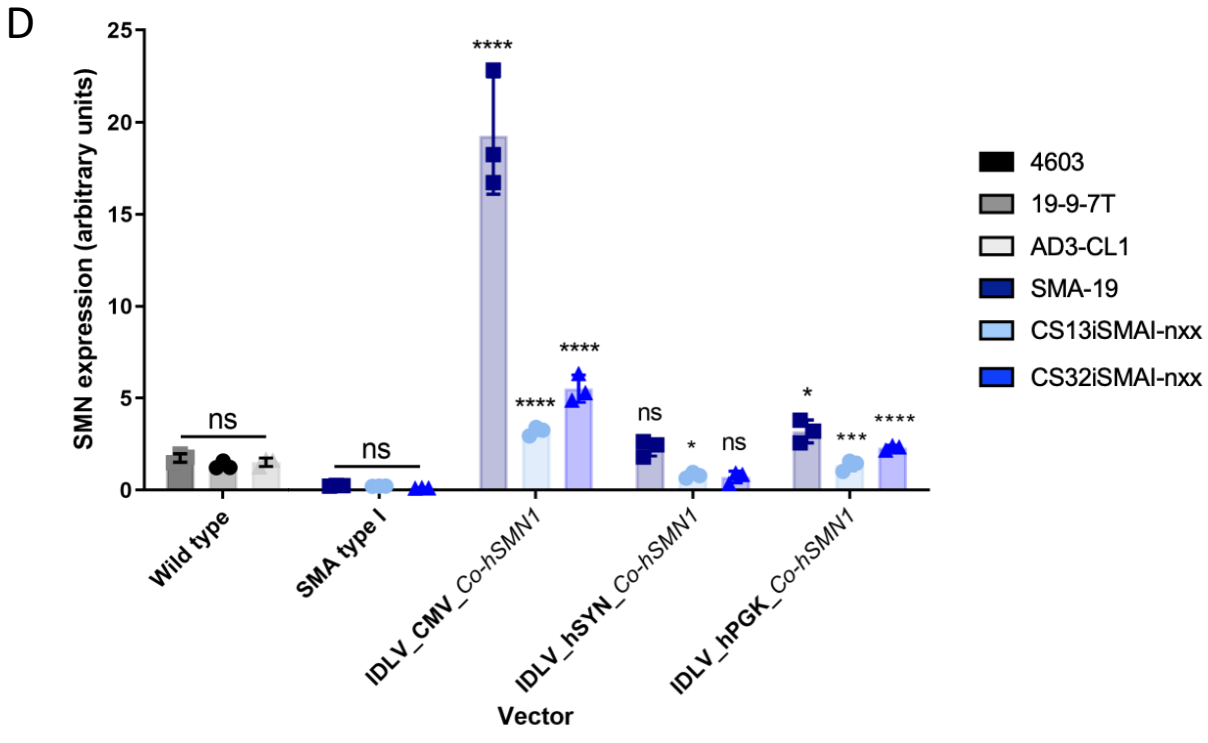
D
SMN expression (arbitrary units)
25
20
15
10
5
0
ns
ns
****
****
****
ns
*
ns
*
***
****
Wild type
SMA type I
IDLV_CMV_Co-hSMN1
IDLV_hSYN_Co-hSMN1
IDLV_hPGK_Co-hSMN1
Vector
4603
19-9-7T
AD3-CL1
SMA-19
CS13iSMAI-nxx
CS32iSMAI-nxx

A

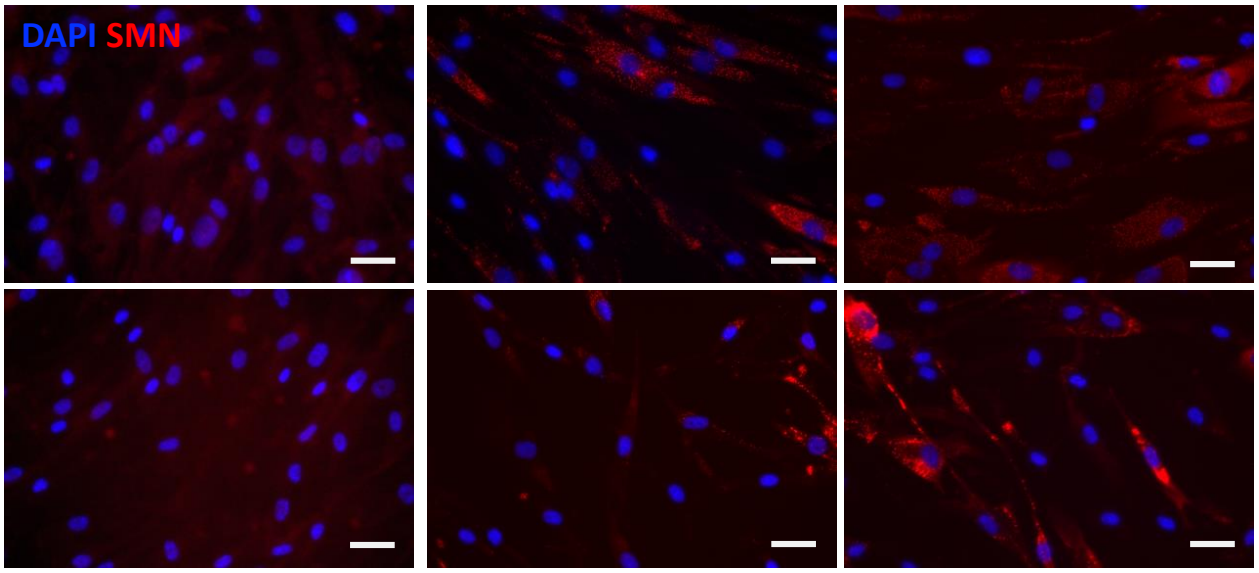
DAPI SMN
Wild type
SMA type I
50 µm
Mock
IDLV_CMV_Co-hSMN1
MOI 75
IDLV_CMV_Co-hSMN1
MOI 100

B

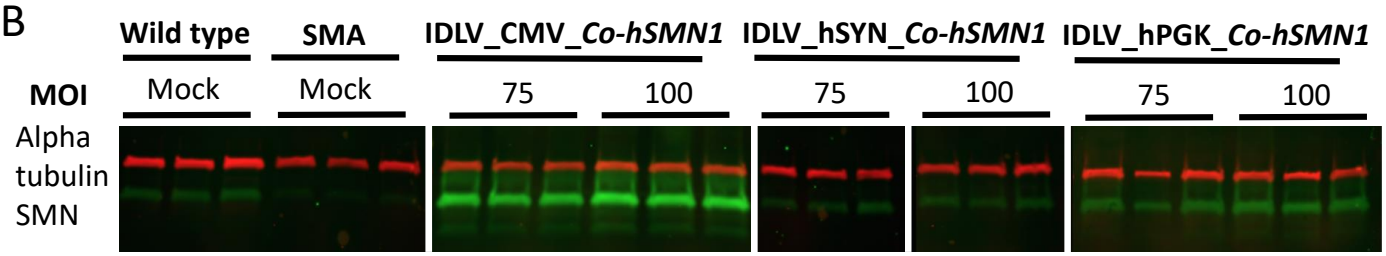
Wild type
SMA
IDLV_CMV_Co-hSMN1
IDLV_hSYN_Co-hSMN1
IDLV_hPGK_Co-hSMN1
MOI
Mock
Mock
75
100
75
100
75
100
Alpha tubulin
SMN

C

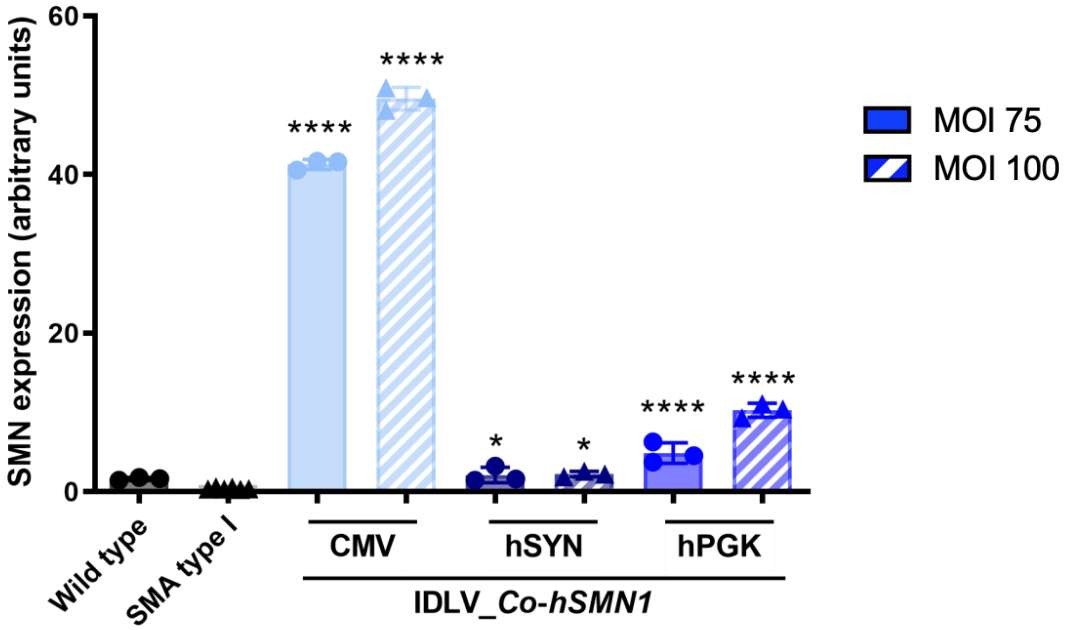
SMN expression (arbitrary units)
60
40
20
0
****
****
*
*
****
****
MOI 75
MOI 100
Wild type
SMA type I
CMV
hSYN
hPGK
IDLV_Co-hSMN1

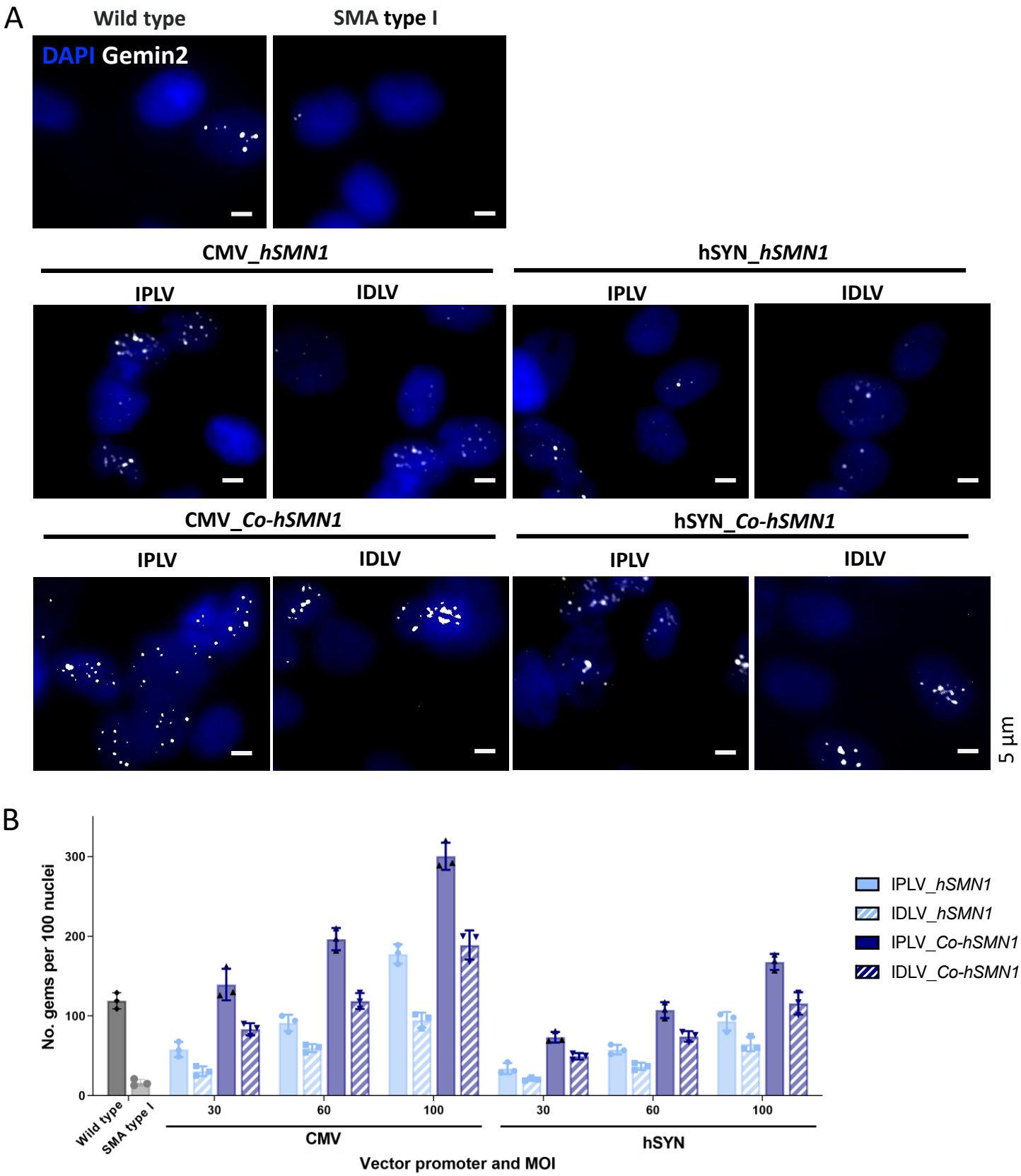
A
Wild type
SMA type I
DAPI Gemin2
CMV_hSMN1
hSYN_hSMN1
IPLV
IDLV
IPLV
IDLV
CMV_Co-hSMN1
hSYN_Co-hSMN1
IPLV
IDLV
IPLV
IDLV
5 µm
B
No. gems per 100 nuclei
300
200
100
0
Wild type
SMA type I
30
60
100
30
60
100
CMV
hSYN
Vector promoter and MOI
IPLV_hSMN1
IDLV_hSMN1
IPLV_Co-hSMN1
IDLV_Co-hSMN1

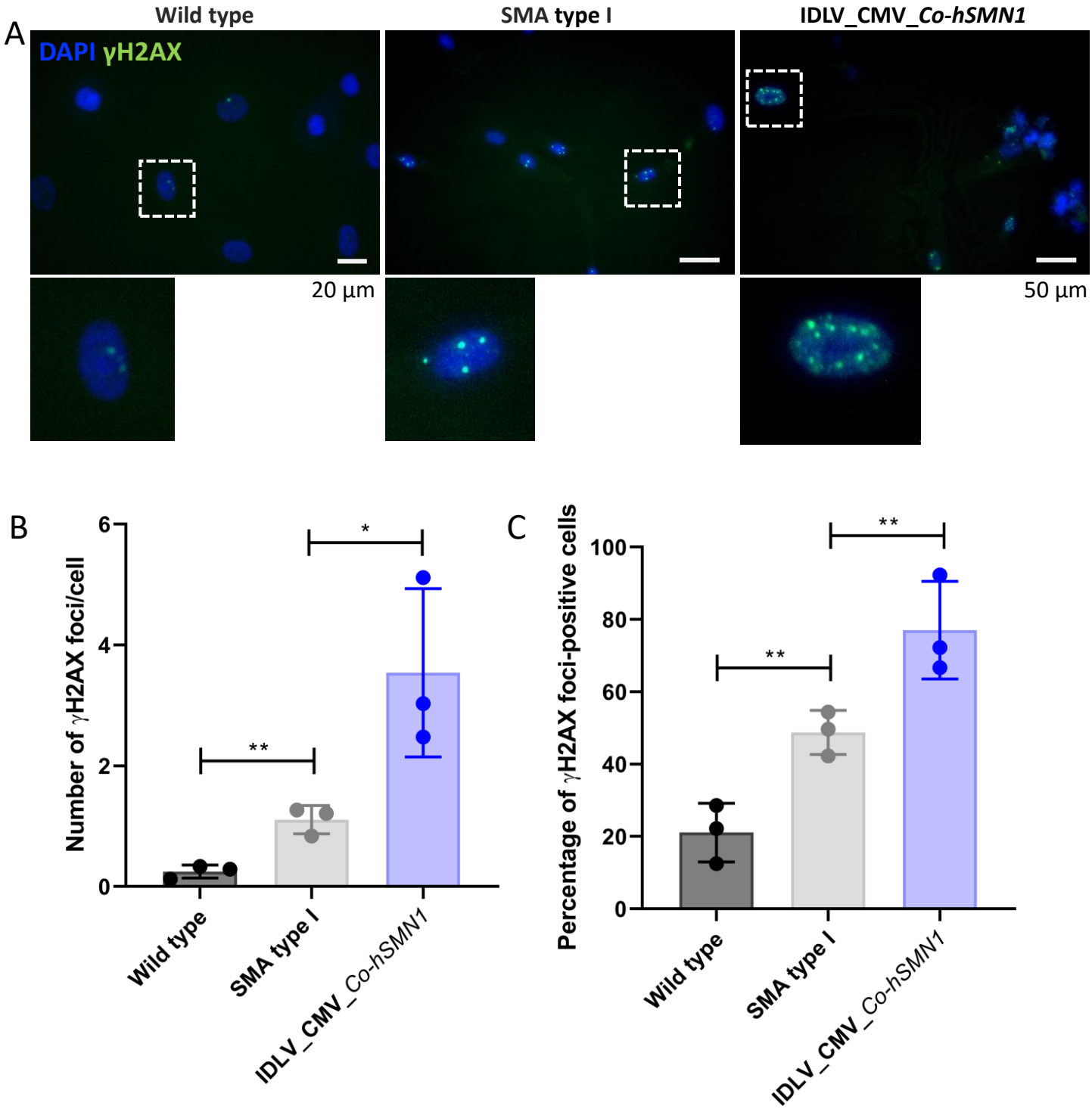
A
Wild type
SMA type I
IDLV_CMV_Co-hSMN1
DAPI γH2AX
20 µm
50 µm
B
Number of γH2AX foci/cell
0
2
4
6
*
**
Wild type
SMA type I
IDLV_CMV_Co-hSMN1
C
Percentage of γH2AX foci-positive cells
0
20
40
60
80
100
**
**
Wild type
SMA type I
IDLV_CMV_Co-hSMN1

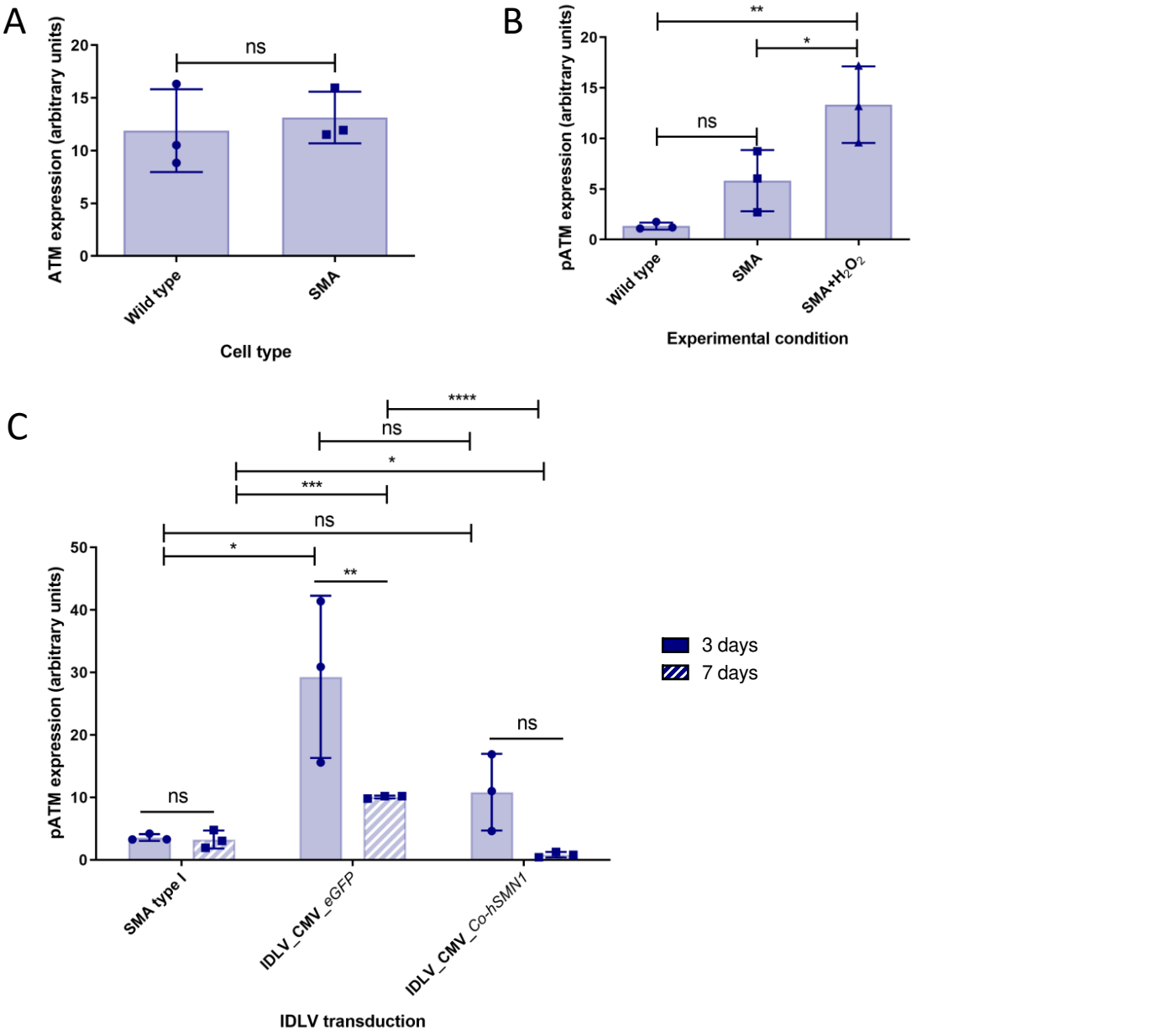
A
ATM expression (arbitrary units)
ns
Wild type
SMA
Cell type
B
pATM expression (arbitrary units)
**
*
ns
Wild type
SMA
SMA+H2O2
Experimental condition
C
pATM expression (arbitrary units)
****
ns
*
***
ns
*
**
ns
ns
SMA type I
IDLV_CMV_eGFP
IDLV_CMV_Co-hSMN1
IDLV transduction
3 days
7 days
D
ATM expression (arbitrary units)
ns
ns
ns
Mock
IDLV_CMV_Co-hSMN1
E
pATM expression (arbitrary units)
****
**
ns
Mock
IDLV_CMV_Co-hSMN1
SMA-19
CS13iSMAI-nxx
CS32iSMAI-nxx

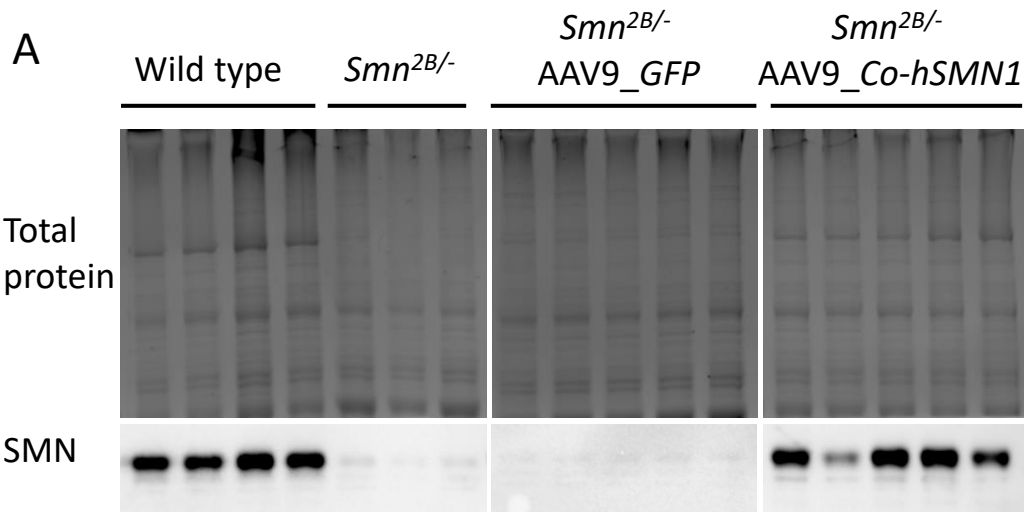
A
Wild type
Smn2B/-
Smn2B/- AAV9_GFP
Smn2B/- AAV9_Co-hSMN1
Total protein
SMN

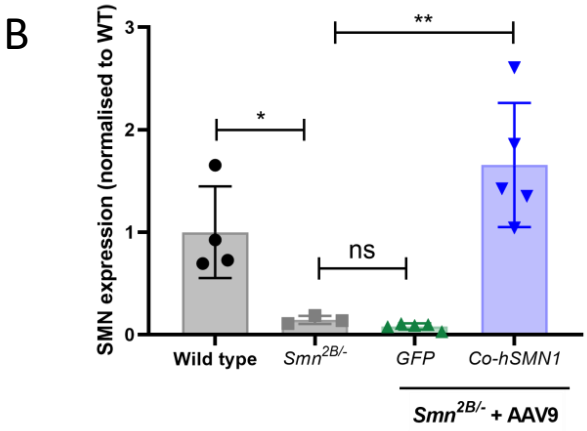
B
SMN expression (normalised to WT)
0
1
2
3
*
**
ns
Wild type
Smn2B/-
GFP
Co-hSMN1
Smn2B/- + AAV9

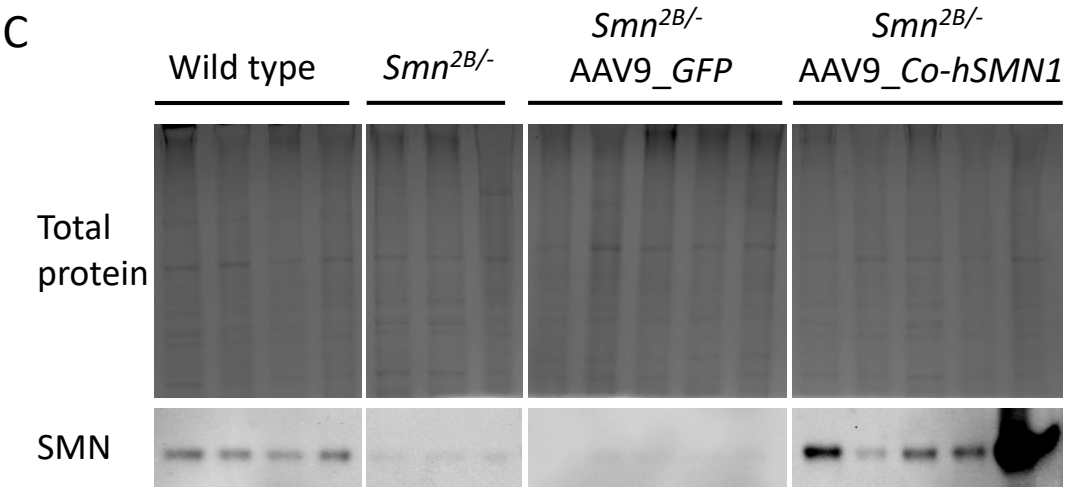
C
Wild type
Smn2B/-
Smn2B/- AAV9_GFP
Smn2B/- AAV9_Co-hSMN1
Total protein
SMN

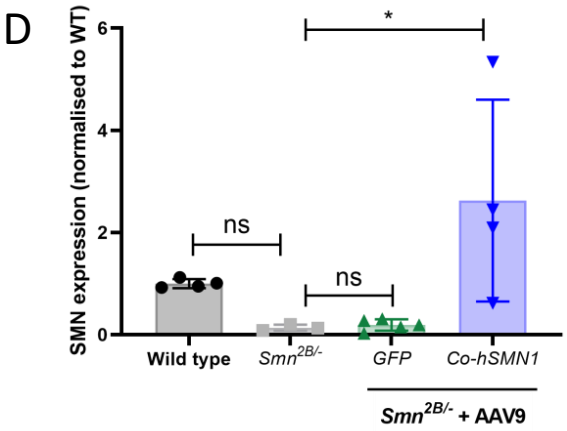
D
SMN expression (normalised to WT)
0
2
4
6
*
ns
ns
Wild type
Smn2B/-
GFP
Co-hSMN1
Smn2B/- + AAV9